

Supporting Information

Highly Selective Hydroboration of Carbonyls by a Manganese Catalyst: Insight into the Reaction Mechanism

Srikanth Vijjamarri, Timothy M. O'Denius, Bin Yao, Alena Kubatova, and Guodong Du*

Department of Chemistry, University of North Dakota, 151 Cornell Street Stop 9024, Grand Forks, North
Dakota 58202, United States

Contents

Experimental Section	4
NMR characterization data	5
Representative Spectra	11
Figure S1: ^{11}B NMR spectrum of DBpin in CD_3CN	11
Figure S2. ^1H NMR spectra of AcPh and reaction progress between AcPh and HBpin	11
Figure S3. ^1H NMR spectra of reaction between <i>p</i> -Cl-AcPh and HBpin	12
Figure S4. ^1H NMR spectra of reaction between <i>p</i> -Br-AcPh and HBpin	12
Figure S5. ^1H NMR spectra of reaction between <i>p</i> -CF ₃ -AcPh and HBpin	13
Figure S6. ^1H NMR spectra of reaction between <i>p</i> -NO ₂ -AcPh and HBpin	13
Figure S7. ^1H NMR spectra of reaction between <i>p</i> -MeO-AcPh and HBpin	14
Figure S8. ^1H NMR spectra of reaction between <i>p</i> -Me-AcPh and HBpin	14
Figure S9. ^1H NMR spectra of reaction between Cyclopropylphenylketone and HBpin	15
Figure S10. ^1H NMR spectra of reaction between Benzophenone and HBpin	15
Figure S11. ^1H NMR spectra of reaction between 2-pentanone and HBpin	16
Figure S12. ^1H NMR spectra of reaction between Cyclohexanone and HBpin	16
Figure S13. ^1H NMR spectra of reaction between 2-cyclohexenone and HBpin	17
Figure S14. ^1H NMR spectra of reaction between PhCHO and HBpin	17
Figure S15. ^1H NMR spectra of reaction between <i>p</i> -MeO-PhCHO and HBpin	18
Figure S16. ^1H NMR spectra of reaction between <i>p</i> -CN-PhCHO and HBpin	18
Figure S17. ^1H NMR spectra of reaction between <i>o</i> -Br-PhCHO and HBpin	19
Figure S18. ^1H NMR spectra of reaction between cyclohexenecarboxaldehyde and HBpin	19
Figure S19. ^1H NMR spectra of reaction between Decanal and HBpin	20
Figure S20. ^1H NMR spectra of reaction between 2-formylpyridine and HBpin	20
Figure S21. ^{11}B NMR spectra of HBpin	21
Figure S22. ^{11}B NMR spectra of reaction between AcPh and HBpin	21
Figure S23. ^{11}B NMR spectra of reaction between <i>p</i> -Cl-AcPh and HBpin	22
Figure S24. ^{11}B NMR spectra of reaction between <i>p</i> -Br-AcPh and HBpin	22
Figure S25. ^{11}B NMR spectra of reaction between <i>p</i> -CF ₃ -AcPh and HBpin	23
Figure S26. ^{11}B NMR spectra of reaction between <i>p</i> -Me-AcPh and HBpin	23
Figure S27. ^{11}B NMR spectra of reaction between 2-cyclohexenone and HBpin	24
Figure S28. ^{11}B NMR spectra of reaction between <i>trans</i> -3-phenyl-2-propenal (cinnamaldehyde) and HBpin	24
Figure S29. ^{11}B NMR spectra of reaction between Cyclohexenecarboxaldehyde and HBpin	25
Figure S30. ^{11}B NMR spectra of reaction between 2-formylpyridine and HBpin	25
Figure S31. ^{13}C NMR spectra of reaction between AcPh and HBpin	26

Figure S32. ^{13}C NMR spectra of reaction between PhCHO and HBpin.....	26
Figure S33. ^{13}C NMR spectra of reaction between <i>p</i> -CN-PhCHO and HBpin	27
Figure S34. ^{13}C NMR spectra of reaction between 2-formylpyridine and HBpin.....	28
Figure S35. ^{13}C NMR spectra of reaction between <i>trans</i> -3-phenyl-2-propenal (cinnamaldehyde) and HBpin	28
Figure S36. ^1H NMR spectra of intermolecular competition between AcPh and PhCHO with HBpin .	29
Figure S37. ^1H NMR spectra of intermolecular competition between <i>p</i> -MeO-AcPh and <i>p</i> -MeO PhCHO with HBpin	29
Figure S38. ^1H NMR spectra of intermolecular competition between <i>p</i> -NO ₂ -AcPh and <i>p</i> -NO ₂ PhCHO with HBpin	30
Figure S39. ^1H NMR spectra of intramolecular chemoselective reaction of acetylbenzaldehyde with HBpin	30
Figure S40. ^1H NMR spectra of competitive reaction between AcPh and <i>p</i> -CH ₃ O-AcPh with HBpin .	31
Figure S41. ^1H NMR spectra of competition reaction between AcPh and <i>p</i> -NO ₂ -AcPh with HBpin....	31
Figure S42. ^1H NMR spectra of competition reaction between AcPh and <i>p</i> -CF ₃ -AcPh with HBpin.....	32
Figure S43. ^{11}B (top) and ^1H (bottom) NMR of catalyst (Mn-1) with HBpin and AcPh.....	33
Figure S44. Reaction scheme of HBcat and DBpin with acetophenone.....	34
Figure S45. ^1H NMR spectra of competition reaction between HBcat and DBpin with acetophenone (5 min).....	34
Figure S46. ^1H NMR spectra of competitive reaction between HBcat and DBpin with acetophenone (1 h).....	35
Figure S47. ^1H NMR spectra of competition reaction between HBcat and DBpin with acetophenone (5 min to 36 h)	35
Figure S48. GC-MS extracted ion chromatograms of reaction between HBpin with acetophenone	36
Figure S49. GC-MS extracted ion chromatograms of competition reaction between HBpin and DBpin with acetophenone	37
Figure S50. ESI-ToF-MS of Mn-1	38
Figure S51. ESI-ToF-MS of reaction products for Mn-1 with HBpin at different ratios.....	39
References.....	40

Experimental Section

Materials and Methods. Deuterated solvents were purchased from the Cambridge Isotope Laboratories and other chemicals were purchased from Millipore Sigma. Solvents were degasified and dried over molecular sieves (4 Å) overnight prior to use. The reagents packed under inert atmosphere were used as received and all other liquid reagents were degasified before use by standard Schlenk line technique. ^1H , ^{13}C , and ^{11}B NMR spectra were recorded on a Bruker AVANCE 500 NMR spectrometer. Boron trifluoride diethyl etherate ($\text{BF}_3\cdot\text{OEt}_2$) was used as the standard reference for ^{11}B NMR analysis.

Gas chromatography mass spectrometry analyses were performed using Agilent GC-MS (6890GC, 5975C) equipped with an autosampler (7386B series) and a split/splitless injector (Agilent Technologies, Santa Clara, CA, USA). Separations were accomplished using a 24.6 m long DB-5 capillary column, 0.25 mm internal diameter (I.D.) and 0.25 mm film thickness (J&W Scientific, Rancho Cordova, CA, USA) at a constant helium flowrate of 1.0 mL/min. Samples (1.0 μL) were injected into a single gooseneck splitless liner with glass wool in a pulsed splitless injection mode with 25 psi for 0.3 min, and solvent delay was set to 2.5 min. The column temperature program started at 35 °C with a hold of 1 min, followed by the gradient of 20 °C/min to 320 °C and hold for 1 min. The MS data (total ion chromatogram, TIC) were acquired in the full scan mode (35–850 m/z) at a scan rate of 1.84 scan/s using the electron ionization (EI) with an electron energy of 70 eV.

High resolution time-of-flight mass spectrometry (HR-ToF-MS) with electrospray ionization (ESI) (G1969A, Agilent Technologies, Santa Clara, CA) was performed in a positive ionization mode. The ESI-HR-ToF-MS analysis was performed by direct infusion at 5 $\mu\text{L}/\text{min}$ using the electrospray (capillary) and fragmentor voltages of 5500 and 250 V, respectively. Nitrogen was used as a nebulizing gas at a flow rate of 4 L/min and drying gas set at 25 psig. All samples for ESI-MS were dissolved in acetonitrile (final concentration of 1 $\mu\text{g}/\text{mL}$) no additional electrolyte was used. The ESI-HR-ToF-MS was calibrated at mass range 100 - 3000 m/z with mass accuracy error < 10 ppm.

General Procedure for the hydroboration of carbonyls. The hydroboration reactions were performed using J. Young NMR tubes in a glovebox under nitrogen atmosphere. Calculated amount of catalyst, **Mn-1**, (0.002 to 1 mol%) was added to 0.35-0.40 mL of CD_3CN at room

temperature. To this was added a carbonyl substrate (0.893 mmol, 1 equiv) followed by hydroborane (0.982 mmol, 1.1 equiv). The progress of the reaction was monitored by the ^1H , ^{13}C , and ^{11}B NMR spectroscopies. After the hydroboration reaction was complete, the reaction mixture was transferred to a round bottom flask/sample vial with acetonitrile and hexane, and hydrolyzed by mixing with aqueous HCl (1 M). After hydrolysis, the organic layer was extracted with hexane and subjected to column chromatography using silica with hexane-EtOAc as eluent. The resultant products were characterized by ^1H and/or ^{13}C NMR and the conversions of the starting carbonyls and the yields of the isolated alcohols were reported in Tables 2 & 3. The identities of the products were confirmed by comparison of ^1H , ^{13}C , and/or ^{11}B NMR spectra with previous literature reports.^{1,2,3}

NMR characterization data

Acetophenone hydroboration product:⁴ ^1H NMR (500 MHz, CD_3CN , 298 K, δ): 1.22 (m, 12H, 4 CH_3), 1.49 (d, 3H, - CH_3), 5.26 (q, 1H, -OCH), 7.28 (m, 1H, - Ph), 7.38 (m, 4H, - Ph). ^{13}C { ^1H } NMR (125 MHz, CD_3CN , 298 K, δ): 25.33 (4 CH_3), 27.08 (CH_3), 73.23 (OCH), 83.51 (-B-OCHpin), 126.18, 128.08, 129.17, 145.65 (Ph). **Hydrolysis product (1-phenylethanol):** ^1H NMR (500 MHz, CDCl_3 , 298 K, δ): 1.42 (d, 3H, CH_3), 4.84 (q, 1H, OCH), 7.18 (d, 2H, Ph), 7.20 (m, 3H, Ph)

Table 2. Entry 1:⁴ ***p*-chloroacetophenone hydroboration product:** ^1H NMR (500 MHz, CD_3CN , 298 K, δ): 1.21 (m, 12H, 4 CH_3), 1.43 (d, 3H, - CH_3), 5.20 (q, 1H, -OCH), 7.31 (m, 4H, - Ph). ^{11}B { ^1H } NMR (99 MHz, CD_3CN , 298 K, δ): 25.40. **Hydrolysis product (1-(4-chlorophenyl)ethanol):** ^1H NMR (500 MHz, CDCl_3 , 298 K, δ): 1.40 (d, 3H, CH_3), 4.89 (q, 1H, OCH), 7.30 (m, 4H, Ph)

Table 2. Entry 2:⁵ ***p*-bromoacetophenone hydroboration product:** ^1H NMR (500 MHz, CD_3CN , 298 K, δ): 1.20 (m, 12H, 4 CH_3), 1.43 (d, 3H, - CH_3), 5.16 (q, 1H, -OCH), 7.25 (m, 2H, - Ph), 7.46 (m, 2H, - Ph). ^{11}B { ^1H } NMR (99 MHz, CD_3CN , 298 K, δ): 25.40. **Hydrolysis product (1-(4-bromophenyl)ethanol):** ^1H NMR (500 MHz, CDCl_3 , 298 K, δ): 1.42 (d, 3H, CH_3), 4.72 (q, 1H, OCH), 7.18 (m, 2H, Ph), 7.42 (m, 2H, Ph)

Table 2. Entry 3:⁴ ***p*-trifluoromethyl acetophenone hydroboration product:** ^1H NMR (500 MHz, CD_3CN , 298 K, δ): 1.20 (m, 12H, 4 CH_3), 1.47 (d, 3H, - CH_3), 5.29 (q, 1H, -OCH), 7.52 (m, 2H, - Ph), 7.64 (m, 2H, - Ph). ^{11}B { ^1H } NMR (99 MHz, CD_3CN , 298 K, δ): 25.42. **Hydrolysis**

product (1-(4-trifluoromethylphenyl)ethanol): ^1H NMR (500 MHz, CDCl_3 , 298 K, δ): 1.51 (d, 3H, CH_3), 4.88 (q, 1H, OCH), 7.44 (m, 2H, *Ph*), 7.57 (m, 2H, *Ph*)

Table 2. Entry 4:⁴ *p*-nitroacetophenone hydroboration product: ^1H NMR (500 MHz, CD_3CN , 298 K, δ): 1.21 (m, 12H, 4 CH_3), 1.46 (d, 3H, CH_3), 5.30 (q, 1H, OCH), 7.55 (d, 2H, *Ph*), 8.16 (d, 2H, *Ph*). **Hydrolysis product (1-(4-nitrophenyl)ethanol):** ^1H NMR (500 MHz, CDCl_3 , 298 K, δ): 1.49 (d, 3H, CH_3), 4.97 (q, 1H, OCH), 7.51 (d, 2H, *Ph*), 8.04 (d, 2H, *Ph*).

Table 2. Entry 5:⁶ *p*-methoxyacetophenone hydroboration product: ^1H NMR (500 MHz, CD_3CN , 298 K, δ): 1.22 (m, 12H, 4 CH_3), 1.45 (d, 3H, CH_3), 3.63 (s, 3H, OCH_3), 5.18 (q, 1H, OCH), 6.88 (d, 2H, *Ph*), 7.27 (d, 2H, *Ph*). ^{11}B { ^1H } NMR (99 MHz, CD_3CN , 298 K, δ): 24.39. **Hydrolysis product (1-(4-methoxyphenyl)ethanol):** ^1H NMR (500 MHz, CDCl_3 , 298 K, δ): 1.50 (d, 3H, CH_3), 3.60 (s, 3H, OCH_3), 4.87 (q, 1H, OCH), 6.88 (d, 2H, *Ph*), 7.27 (d, 2H, *Ph*).

Table 2. Entry 6:⁷ *p*-methylacetophenone hydroboration product: ^1H NMR (500 MHz, CD_3CN , 298 K, δ): 1.22 (m, 12H, 4 CH_3), 1.47 (d, 3H, CH_3), 2.33 (s, 3H, CH_3), 5.22 (q, 1H, OCH), 7.16 (d, 2H, *Ph*), 7.26 (d, 2H, *Ph*). ^{11}B { ^1H } NMR (99 MHz, CD_3CN , 298 K, δ): 24.49. **Hydrolysis product (1-(4-methylphenyl)ethanol):** ^1H NMR (500 MHz, CDCl_3 , 298 K, δ): 1.41 (d, 3H, CH_3), 2.25 (s, 3H, CH_3), 4.82 (q, 1H, OCH), 7.08 (d, 2H, *Ph*), 7.15 (d, 2H, *Ph*).

Table 2. Entry 7:⁶ cyclopropylphenylketone hydroboration product: ^1H NMR (500 MHz, CD_3CN , 298 K, δ): 0.40-0.50 (m, 4H, cyclopropyl 2 CH_2), 1.21 (m, 1H, cyclopropyl CH), 1.23 (m, 12H, 4 CH_3), 4.49 (m, 1H, OCH), 7.28 (m, 1H, *Ph*), 7.36 (m, 2H, *Ph*), 7.41 (m, 2H, *Ph*). **Hydrolysis product (α -cyclopropylbenzylalcohol):** ^1H NMR (500 MHz, CDCl_3 , 298 K, δ): 0.35-0.46 (m, 4H, cyclopropyl 2 CH_2), 0.56 (m, 1H, cyclopropyl CH), 4.02 (m, 1H, OCH), 7.20 (m, 1H, *Ph*), 7.31 (m, 2H, *Ph*), 7.48 (m, 2H, *Ph*)

Table 2. Entry 8:⁶ benzophenone hydroboration product: ^1H NMR (500 MHz, CD_3CN , 298 K, δ): 1.26 (m, 12H, 4 CH_3), 6.30 (s, 1H, OCH), 7.31 (m, 2H, *Ph*), 7.39 (m, 4H, *Ph*), 7.48 (m, 4H, *Ph*). **Hydrolysis product (α -phenylbenzenemethanol):** ^1H NMR (500 MHz, CDCl_3 , 298 K, δ): 2.37 (s, 1H, OH), 5.81 (s, 1H, OCH), 7.28 (m, 2H, *Ph*), 7.33 (m, 4H, *Ph*), 7.37 (m, 4H, *Ph*)

Table 2. Entry 9:⁸ 2-pentanone hydroboration product: ^1H NMR (500 MHz, CD_3CN , 298 K, δ): 0.89 (m, 3H, CH_3), 1.13 (m, 2H, CH_2), 1.23 (m, 12H, 4 CH_3), 1.35 (m, 3H, OCHCH_3), 1.43 (m, 2H, OCHCH_2), 4.11 (m, 1H, OCH)

Table 2. Entry 10:⁸ **cyclohexanone hydroboration product:** ¹H NMR (500 MHz, CD₃CN, 298 K, δ): 1.19 (m, 12H, 4CH₃), 1.25 (m, 4H, CH₂), 1.49 (m, 2H, CH₂), 1.69 (m, 2H, CH₂), 1.78 (m, 2H, CH₂), 3.90 (m, 1H, OCH)

Table 2. Entry 11:⁸ **3-cyclohexenone hydroboration product:** ¹H NMR (500 MHz, CD₃CN, 298 K, δ): 1.25 (m, 12H, 4CH₃), 1.65 (m, 2H, CH₂), 1.79 (m, 1H, CH), 1.91 (m, 1H, CH), 2.03 (m, 2H, CH₂), 4.58 (m, 1H, OCH), 5.73 (m, 1H, CH=CH), 5.88 (m, 1H, CH=CH). ¹¹B {¹H} NMR (99 MHz, CD₃CN, 298 K, δ): 25.17. **Hydrolysis product (3-cyclohexene-1-methanol):** ¹H NMR (500 MHz, CDCl₃, 298 K, δ): 1.58-2.36 (m, 6H, 3CH₂), 4.45 (m, 1H, OCH), 5.62 (m, 1H, CH=CH), 5.71 (m, 1H, CH=CH)

Table 2. Entry 12:⁷ **benzylideneacetophenone hydroboration product:** ¹H NMR (500 MHz, CD₃CN, 298 K, δ): 1.26 (m, 12H, 4CH₃), 5.81 (m, 1H, -OCH), 6.44 (m, 1H, -OCHCH=CH), 6.74 (m, 1H, -OCHCH=CH), 7.26-7.56 (m, 10H, Ph). ¹¹B {¹H} NMR (99 MHz, CD₃CN, 298 K, δ): 26.10. **Hydrolysis product (1,3-diphenyl-2-propen-1-ol):** ¹H NMR (500 MHz, CDCl₃, 298 K, δ): 5.20 (m, 1H, -OCH), 6.35 (m, 1H, -OCHCH=CH), 6.68 (m, 1H, -OCHCH=CH), 7.18-7.46 (m, 10H, -Ph)

Table 2. Entry 13:⁹ **4-phenyl-3-butyne-2-one hydroboration product:** ¹H NMR (500 MHz, CD₃CN, 298 K, δ): 1.24 (m, 12H, 4CH₃), 1.52 (d, 3H, -CH₃), 5.05 (q, 1H, -OCH), 7.35 (m, 3H, -Ph), 7.42 (m, 2H, -Ph). ¹³C {¹H} NMR (125 MHz, CD₃CN, 298 K, δ): 24.30 (4CH₃), 24.92 (4CH₃), 61.97 (-OCH), 83.87 (4° C of Bpin), 84.19 (-OCHC≡C), 90.89 (-OCHC≡CPh), 129.43, 129.73, 132.32, 133.75 (Ph). ¹¹B {¹H} NMR (99 MHz, CD₃CN, 298 K, δ): 25.48. **Hydrolysis product (4-phenyl-3-butyne-2-ol):** ¹H NMR (500 MHz, CDCl₃, 298 K, δ): 1.46 (m, 3H, -CH₃), 4.84 (m, 1H, -OCH), 7.29 (m, 2H, -Ph), 7.31 (m, 3H, -Ph)

Table 3. Entry 1 & 3:⁶ **benzaldehyde hydroboration product:** ¹H NMR (500 MHz, CD₃CN, 298 K, δ): 1.21 (m, 12H, 4CH₃), 4.85 (s, 2H, OCH₂), 6.95 (d, 2H, Ph), 7.31 (d, 2H, Ph). ¹³C {¹H} NMR (125 MHz, CD₃CN, 298 K, δ): 25.03 (4CH₃), 67.35 (OCH₂), 83.76 (B-OCHpin), 127.68, 128.37, 129.32, 140.51 (Ph). ¹¹B {¹H} NMR (99 MHz, CD₃CN, 298 K, δ): 24.05. **Hydrolysis product (benzyl alcohol)** ¹H NMR (500 MHz, CDCl₃, 298 K, δ): 4.68 (s, 2H, OCH₂), 7.19 (m, 2H, Ph), 7.35-7.40 (m, 3H, Ph)

Table 3. Entry 2 & 4:⁶ *p*-methoxybenzaldehyde hydroboration product: ¹H NMR (500 MHz, CD₃CN, 298 K, δ): 1.26 (m, 12H, 4CH₃), 3.78 (s, 3H, OCH₃), 4.83 (s, 2H, OCH₂), 6.92 (d, 2H, *Ph*), 7.29 (d, 2H, *Ph*). **Hydrolysis product** (*p*-methoxybenzyl alcohol) ¹H NMR (500 MHz, CDCl₃, 298 K, δ): 3.52 (s, 3H, OCH₃), 4.61 (s, 2H, OCH₂), 6.82 (m, 2H, *Ph*), 7.11 (m, 2H, *Ph*).

Table 3. Entry 5:⁶ *p*-nitro benzaldehyde hydroboration product: ¹H NMR (500 MHz, CD₃CN, 298 K, δ): 1.23 (m, 12H, 4CH₃), 4.98 (s, 3H, OCH), 7.52 (d, 2H, *Ph*), 8.17 (d, 2H, *Ph*). **Hydrolysis product** (*p*-nitrobenzyl alcohol) ¹H NMR (500 MHz, CDCl₃, 298 K, δ): 4.81 (s, 2H, OCH₂), 7.45 (m, 2H, *Ph*), 8.09 (m, 2H, *Ph*).

Table 3. Entry 6:⁷ *p*-cyanobenzaldehyde hydroboration product: ¹H NMR (500 MHz, CD₃CN, 298 K, δ): 1.23 (m, 12H, 4CH₃), 4.93 (m, 2H, OCH₂), 7.46 (m, 2H, *Ph*), 7.69 (m, 2H, *Ph*). ¹³C {¹H} NMR (125 MHz, CD₃CN, 298 K, δ): 24.92 (4CH₃), 66.44 (OCH₂), 83.99 (B-OCHpin), 111.76, 127.90, 133.16, 145.89 (*Ph*). **Hydrolysis product** (*p*-cyanobenzyl alcohol) ¹H NMR (500 MHz, CDCl₃, 298 K, δ): 4.76 (s, 2H, OCH₂), 7.42 (m, 2H, *Ph*), 7.62 (m, 2H, *Ph*)

Table 3. Entry 7:⁴ *p*-chlorobenzaldehyde hydroboration product: ¹H NMR (500 MHz, CD₃CN, 298 K, δ): 1.22 (m, 12H, 4CH₃), 4.96 (m, 2H, OCH₂), 7.45 (m, 2H, *Ph*), 7.62 (m, 2H, *Ph*). ¹¹B {¹H} NMR (99 MHz, CD₃CN, 298 K, δ): 24.92. **Hydrolysis product** (*p*-chlorobenzyl alcohol) ¹H NMR (500 MHz, CDCl₃, 298 K, δ): 4.69 (s, 2H, OCH₂), 7.39 (m, 2H, *Ph*), 7.50 (m, 2H, *Ph*)

Table 3. Entry 8:⁶ *p*-bromobenzaldehyde hydroboration product: ¹H NMR (500 MHz, CD₃CN, 298 K, δ): 1.23 (m, 12H, 4CH₃), 4.95 (m, 2H, OCH₂), 7.43 (m, 2H, *Ph*), 7.65 (m, 2H, *Ph*). ¹¹B {¹H} NMR (99 MHz, CD₃CN, 298K, δ): 24.95. **Hydrolysis product** (*p*-bromobenzyl alcohol) ¹H NMR (500 MHz, CDCl₃, 298 K, δ): 4.55 (s, 2H, OCH₂), 7.22 (m, 2H, *Ph*), 7.37 (m, 2H, *Ph*)

Table 3. Entry 9:⁷ *o*-bromo benzaldehyde hydroboration product: ¹H NMR (500 MHz, CD₃CN, 298 K, δ): 1.24 (m, 12H, 4CH₃), 4.93 (s, 3H, OCH), 7.19 (m, 1H, *Ph*), 7.36 (m, 1H, *Ph*), 7.47 (m, 1H, *Ph*), 7.54 (d, 1H, *Ph*). **Hydrolysis product** (*o*-bromobenzyl alcohol) ¹H NMR (500 MHz, CDCl₃, 298 K, δ): 4.72 (s, 2H, OCH₂), 7.11 (m, 1H, *Ph*), 7.28 (m, 1H, *Ph*), 7.41 (m, 1H, *Ph*), 7.48 (m, 1H, *Ph*)

Table 3. Entry 10:⁷ *trans*-3-phenyl-2-propenal hydroboration product (cinnamaldehyde): ¹H NMR (500 MHz, CD₃CN, 298 K, δ): 1.29 (m, 12H, 4CH₃), 4.65 (m, 2H, OCH₂), 6.34 (m, 1H, -CH=CHPh), 6.36 (m, 1H, -CH=CHPh), 7.23-7.29 (m, 3H, Ph), 7.41 (m, 2H, Ph). ¹³C {¹H} NMR (125 MHz, CD₃CN, 298 K, δ): 24.30 (4CH₃), 25.01 (4CH₃), 65.85 (-OCH₂), 83.57 (-OCH₂), 131.30 (CH=CHPh), 153.43 (CH=CHPh), 127.26, 128.52, 128.50, 137.67 (Ph). ¹¹B {¹H} NMR (99 MHz, CD₃CN, 298 K, δ): 25.60. **Hydrolysis product** (cinnamyl alcohol): ¹H NMR (500 MHz, CDCl₃, 298 K, δ): 4.12 (s, 2H, OCH₂), 6.20 (m, 1H, -CH=CHPh), 6.34 (m, 1H, -CH=CHPh), 7.01 (m, 2H, Ph), 7.08-7.17 (m, 3H, Ph)

Table 3. Entry 11:⁴ 3-cyclohexenecarboxaldehyde hydroboration product: ¹H NMR (500 MHz, CD₃CN, 298 K, δ): 1.21 (m, 12H, 4CH₃), 1.27 (m, 4H, CH₂), 2.03 (m, 3H, CH & CH=CH), 3.67 (m, 2H, OCH₂), 5.64 (m, 2H, -OCH₂). ¹¹B {¹H} NMR (99 MHz, CD₃CN, 298 K, δ): 25.32. **Hydrolysis product** (3-cyclohexene-1-methanol) ¹H NMR (500 MHz, CDCl₃, 298 K, δ): 1.25-2.52 (m, 6H, CH₂), 3.56 (m, 2H, OCH₂), 5.61 (m, 2H, CH=CH)

Table 3. Entry 12:⁶ 1-Decanal hydroboration product: ¹H NMR (500 MHz, CD₃CN, 298 K, δ): 0.89 (m, 3H, CH₃), 1.22 (m, 12H, 4CH₃), 1.27 (m, 14H, 7CH₂), 1.56 (m, 2H, CH₂), 3.60 (m, 2H, OCH₂).

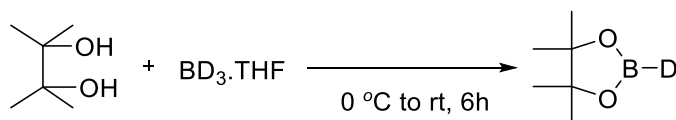
Table 3. Entry 13:⁴ 2-formylpyridine hydroboration product: ¹H NMR (500 MHz, CD₃CN, 298 K, δ): 1.22 (m, 12H, 4CH₃), 4.92 (s, 2H, OCH₂), 7.38 (m, 1H, pyridine), 7.46 (m, 1H, pyridine), 7.87 (m, 1H, pyridine), 8.54 (m, 1H, pyridine). ¹³C {¹H} NMR (125 MHz, CD₃CN, 298 K, δ): 25.58 (4CH₃), 67.25 (-OCH₂), 82.19 (-B-OCpin), 121.17 (pyridine), 124.06 (pyridine), 139.49 (pyridine), 146.29 (pyridine), 149.99 (pyridine). ¹¹B {¹H} NMR (99 MHz, CD₃CN, 298 K, δ): 21.25. **Hydrolysis product** (2-pyridinemethanol) ¹H NMR (500 MHz, CDCl₃, 298 K, δ): 4.78 (s, 2H, OCH₂), 7.31 (m, 1H, pyridine), 7.39 (m, 1H, pyridine), 7.81 (m, 1H, pyridine), 8.42 (m, 1H, pyridine)

Table 3. Entry 14:⁷ furfural hydroboration product: ¹H NMR (500 MHz, CD₃CN, 298 K, δ): 1.26 (m, 12H, 4CH₃), 4.80 (s, 2H, OCH₂), 6.32-6.36 (m, 2H, furan ring), 7.48 (m, 1H, furan ring). **Hydrolysis product** (2-furanmethanol) ¹H NMR (500 MHz, CDCl₃, 298 K, δ): 4.72 (s, 2H, OCH₂), 6.01 (m, 1H, furan ring), 6.32 (m, 1H, furan ring), 7.33 (m, 1H, furan ring)

Table 3. Entry 15:⁶ **thiophene-2-carboxaldehyde hydroboration product:** ¹H NMR (500 MHz, CD₃CN, 298 K, δ): 1.29 (m, 12H, 4CH₃), 5.04 (s, 2H, OCH₂), 7.02-7.06 (m, 2H, *thiophene ring*), 7.36 (m, 1H, *thiophene ring*). **Hydrolysis product** (2-thiophenemethanol) ¹H NMR (500 MHz, CDCl₃, 298 K, δ): 4.82 (s, 2H, OCH₂), 6.98 (m, 1H, *thiophene ring*), 7.01 (m, 1H, *thiophene ring*), 7.28 (m, 1H, *thiophene ring*)

Acetylbenzaldehyde hydroboration products:^{4,7} ¹H NMR (500 MHz, CD₃CN, 298 K, δ): (**Aldehyde group reduction only**) 1.24 (m, 12H, 4CH₃), 2.54 (s, 3H, COCH₃), 4.94 (s, 2H, -OCH₂), 7.42 (m, 2H, *Ph*), 7.93 (m, 2H, *Ph*). ¹³C {¹H} NMR (125 MHz, CDCl₃, 298 K, δ): 24.30 (4CH₃), 27.36 (unreacted CH₃), 66.65 (-OCH₂), 84.12 (4° C of Bpin), 127.27, 129.25, 130.46, 145.57 (*Ph*), 129.15, 129.57, 133.96, 138.20 (unreacted *Ph*), 198.28 (unreacted CO of ketone group). After **2nd equivalent of HBpin was added**, both aldehyde and ketone **groups were reduced:** 1.20 (m, 24H, 4CH₃), 1.40 (m, 3H, OCHCH₃), 4.89 (m, 2H, -OCH₂), 5.26 (m, 1H, -OCH), 7.33 (m, 4H, *Ph*). **Hydrolysis product (α-methyl-1,4-benzenedimethanol)** ¹H NMR (500 MHz, CDCl₃, 298 K, δ): 1.43 (m, 3H, CHCH₃), 4.96 (m, 2H, -OCH₂), 5.23 (m, 1H, -OCH), 7.25-7.32 (m, 4H, *Ph*).

Synthesis of DBpin



This procedure was adapted from the literature.¹⁰ BD₃•THF (2 mmol, 1M in THF) solution was placed in a Schlenk flask equipped with a stir bar under nitrogen. After cooling to 0 °C using an ice bath, pinacol (2 mmol) was then added slowly and the solution was allowed to warm to rt and stirred for 6 hours. The resulting solution was stripped off excess THF by using Schlenk technique. ¹H and ¹¹B NMR spectroscopy confirmed the formation of deuterated pinacolborane.

Representative Spectra

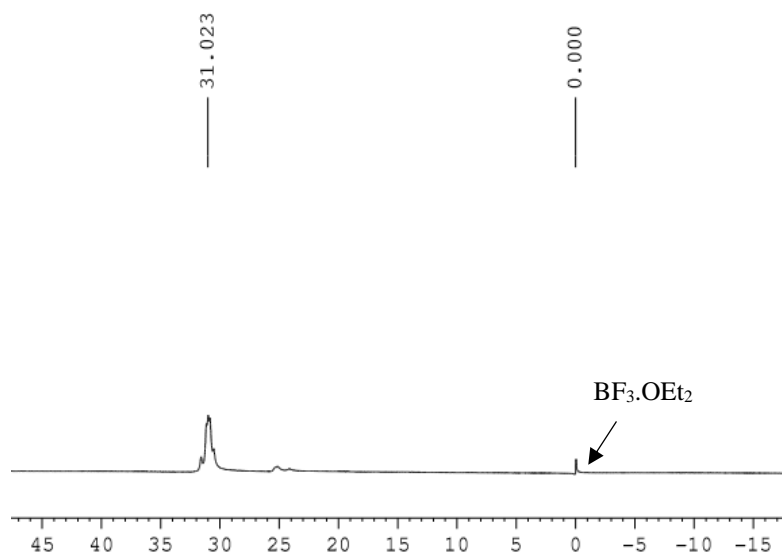


Figure S1: ^{11}B NMR spectrum of DBpin in CD_3CN

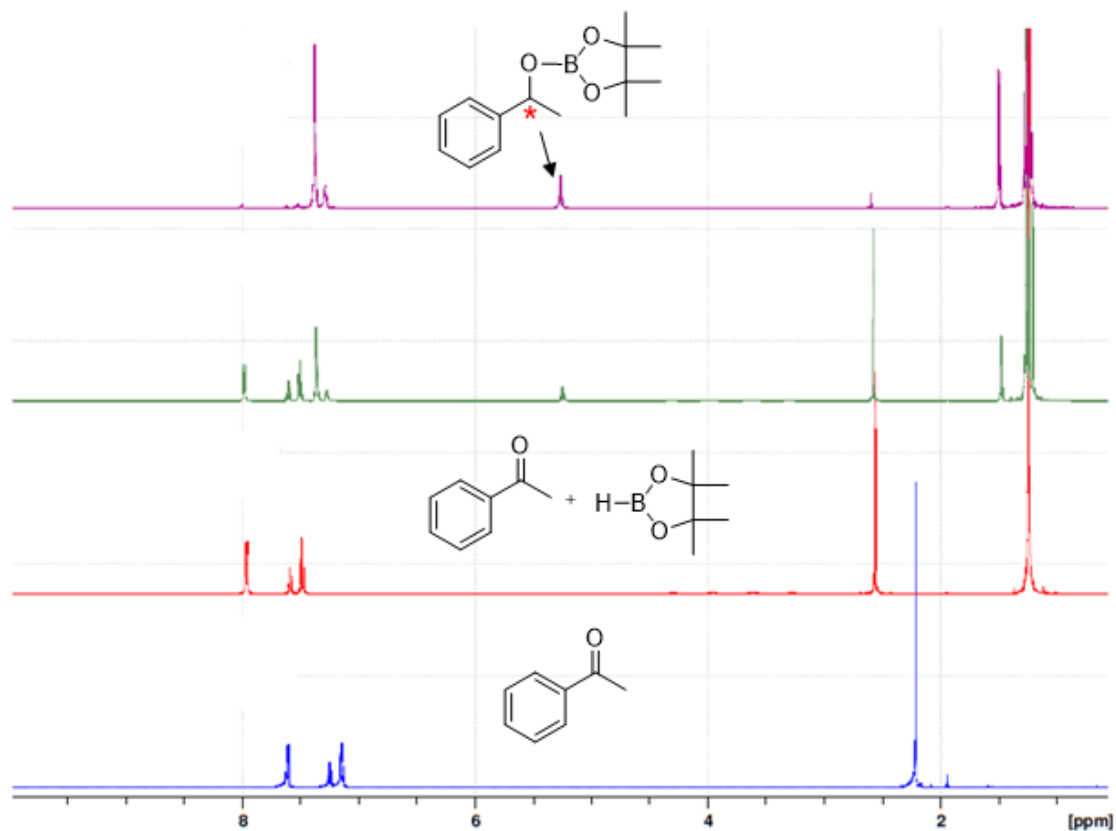


Figure S2. ^1H NMR spectra of AcPh and reaction progress between AcPh and HBpin

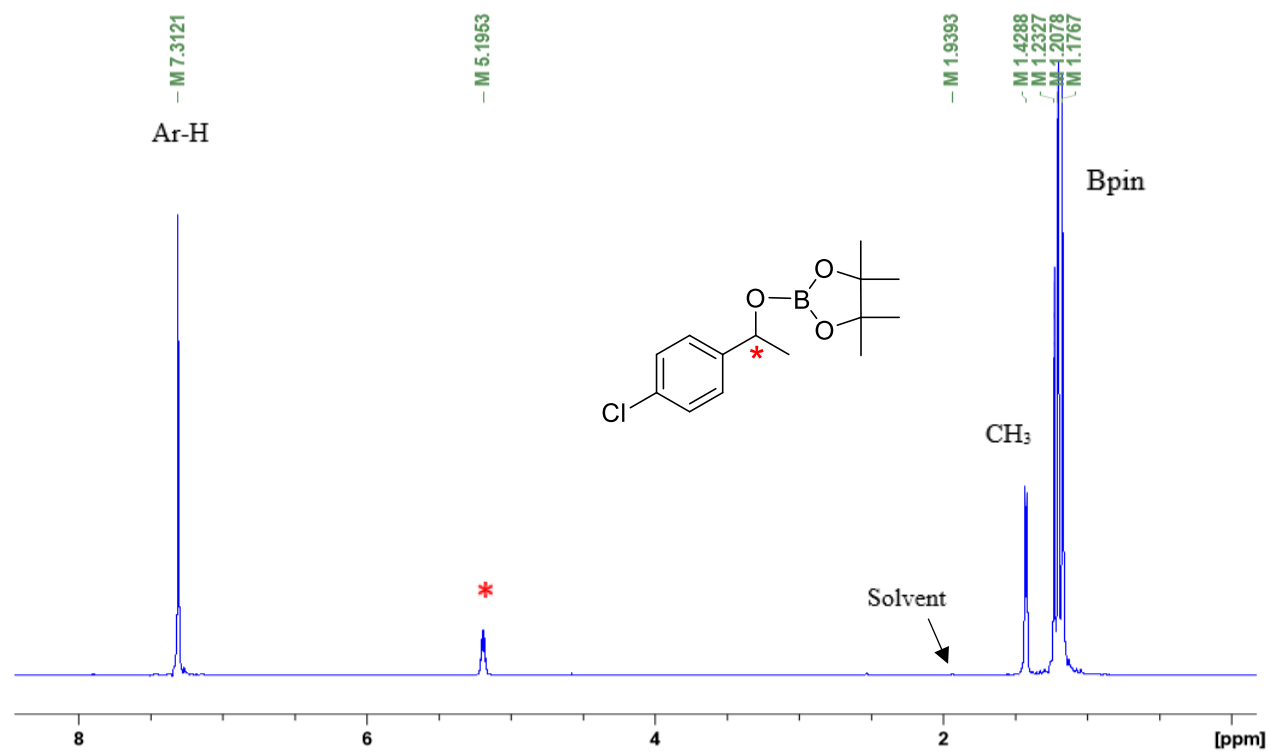


Figure S3. ¹H NMR spectra of reaction between *p*-Cl-AcPh and HBpin

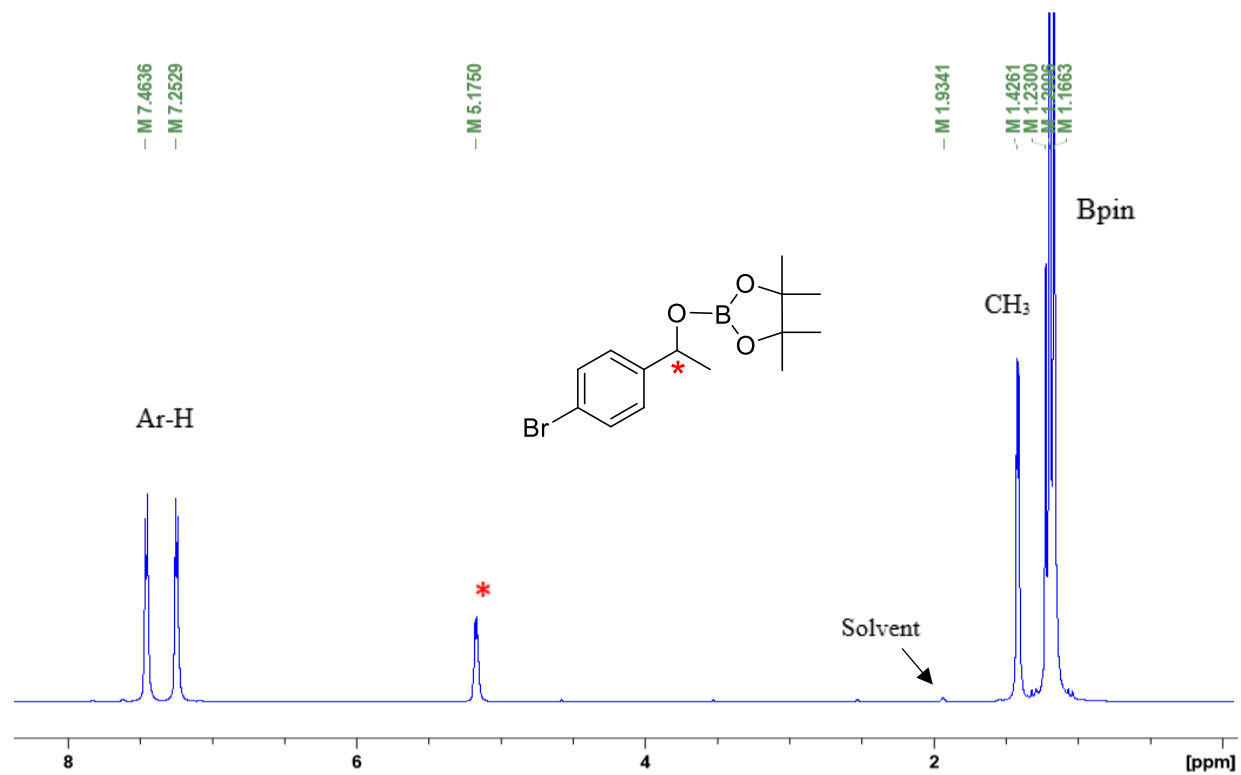


Figure S4. ¹H NMR spectra of reaction between *p*-Br-AcPh and HBpin

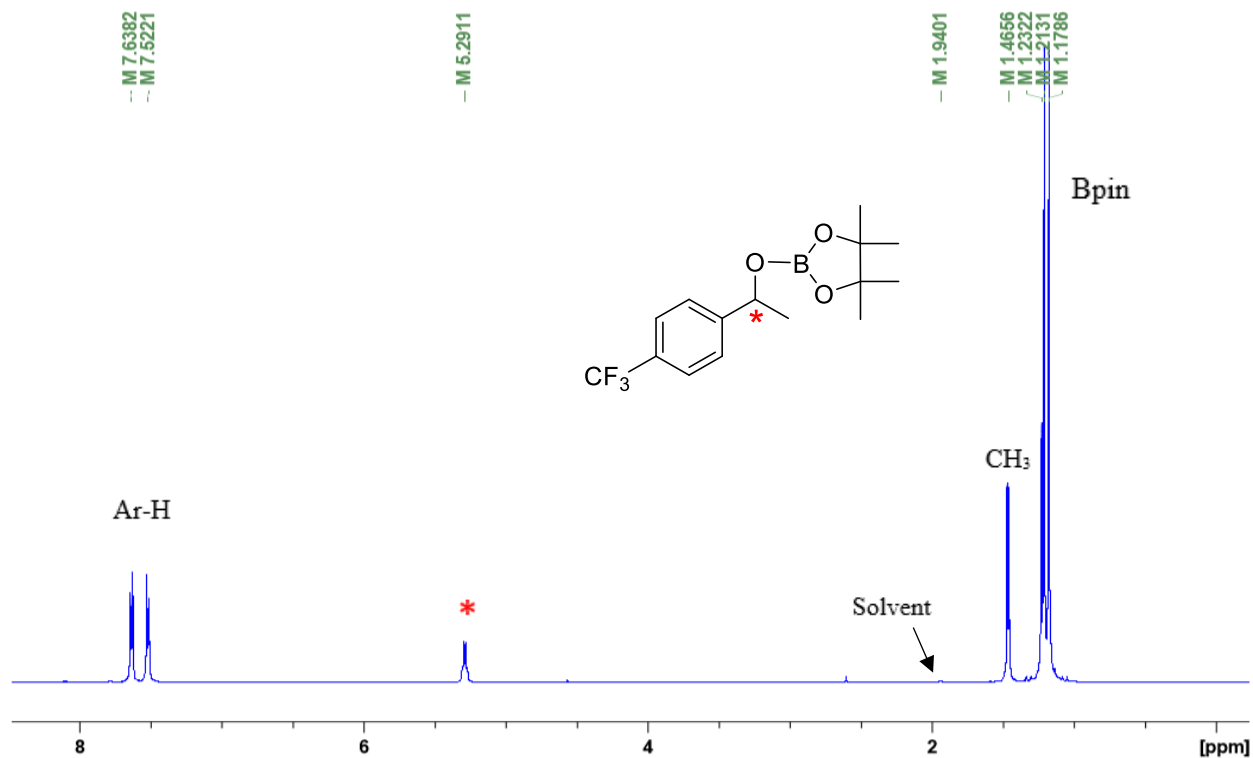


Figure S5. ¹H NMR spectra of reaction between *p*-CF₃-AcPh and HBpin

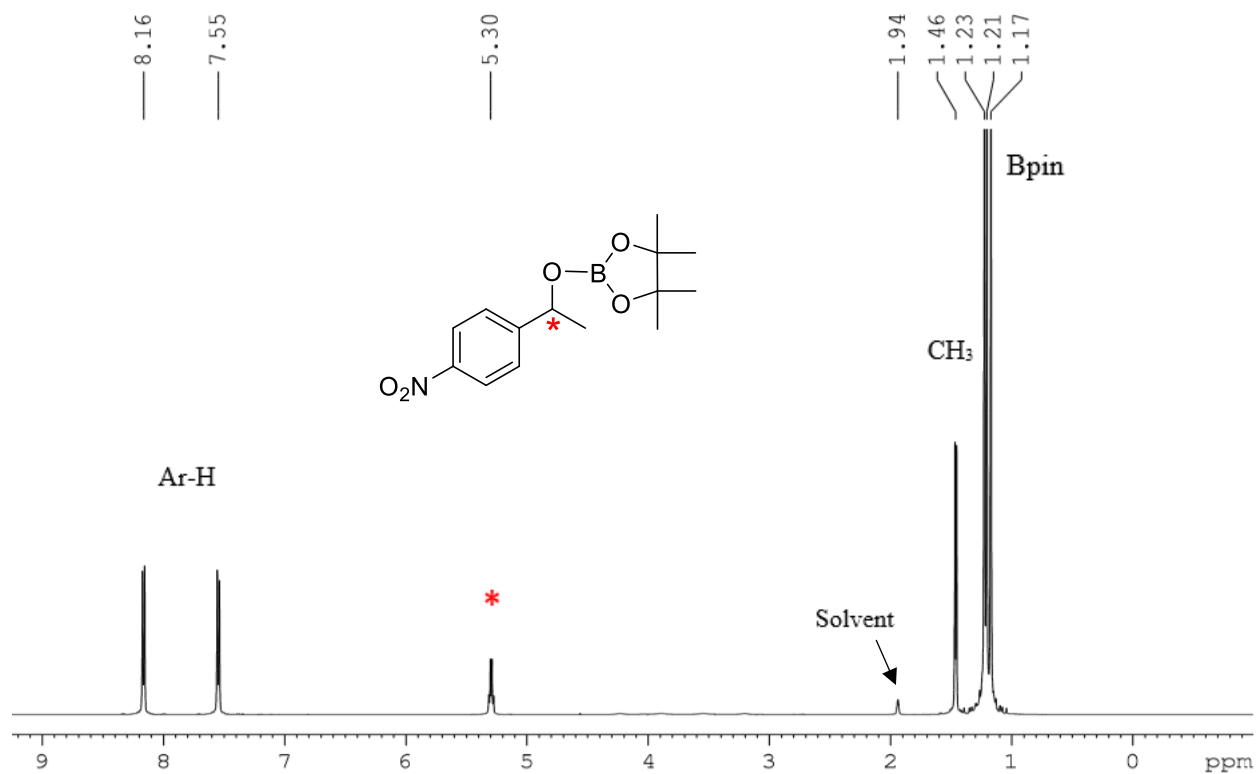


Figure S6. ¹H NMR spectra of reaction between *p*-NO₂-AcPh and HBpin

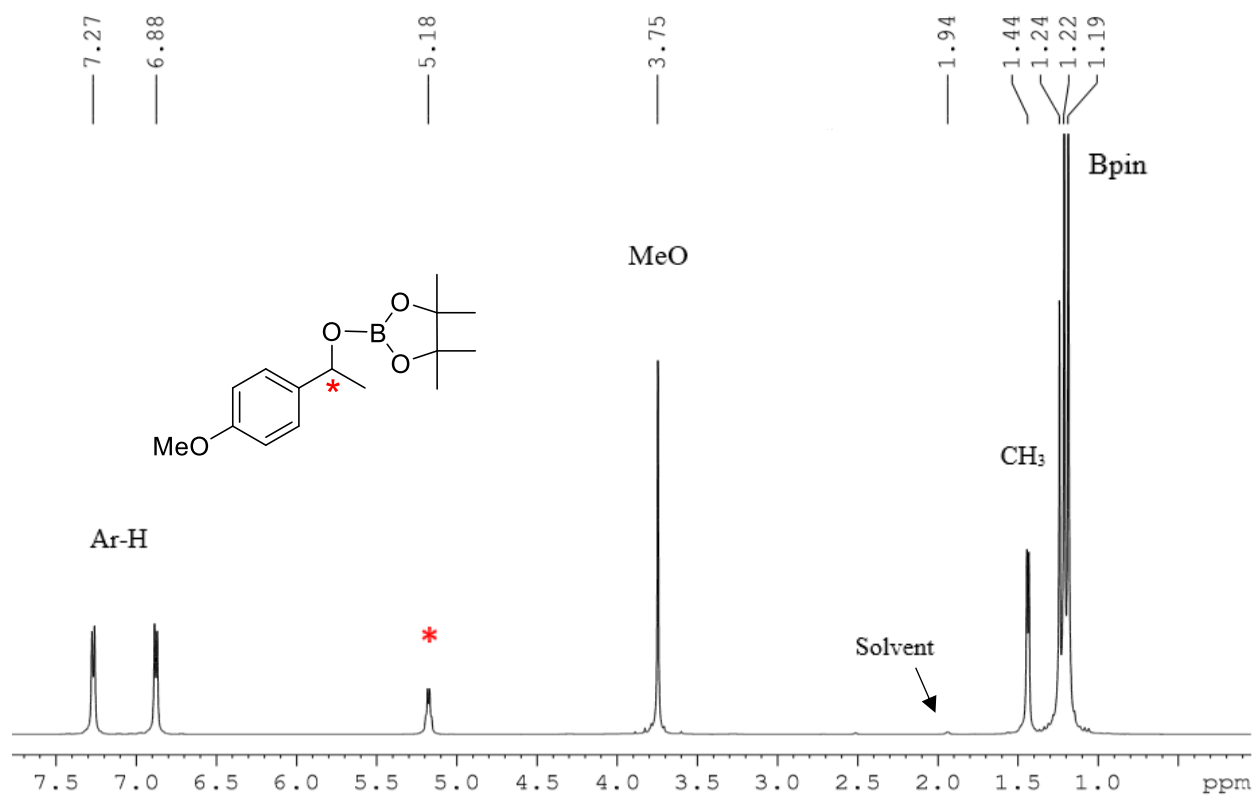


Figure S7. ¹H NMR spectra of reaction between *p*-MeO-AcPh and HBpin

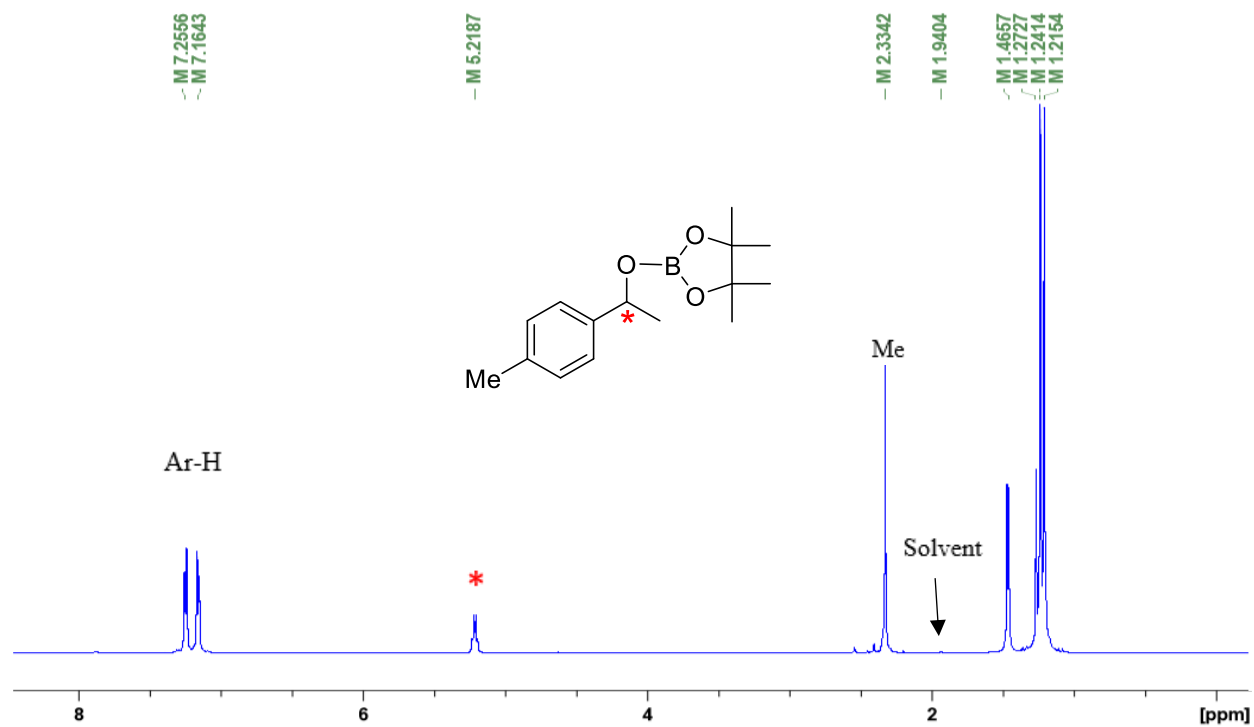


Figure S8. ¹H NMR spectra of reaction between *p*-Me-AcPh and HBpin

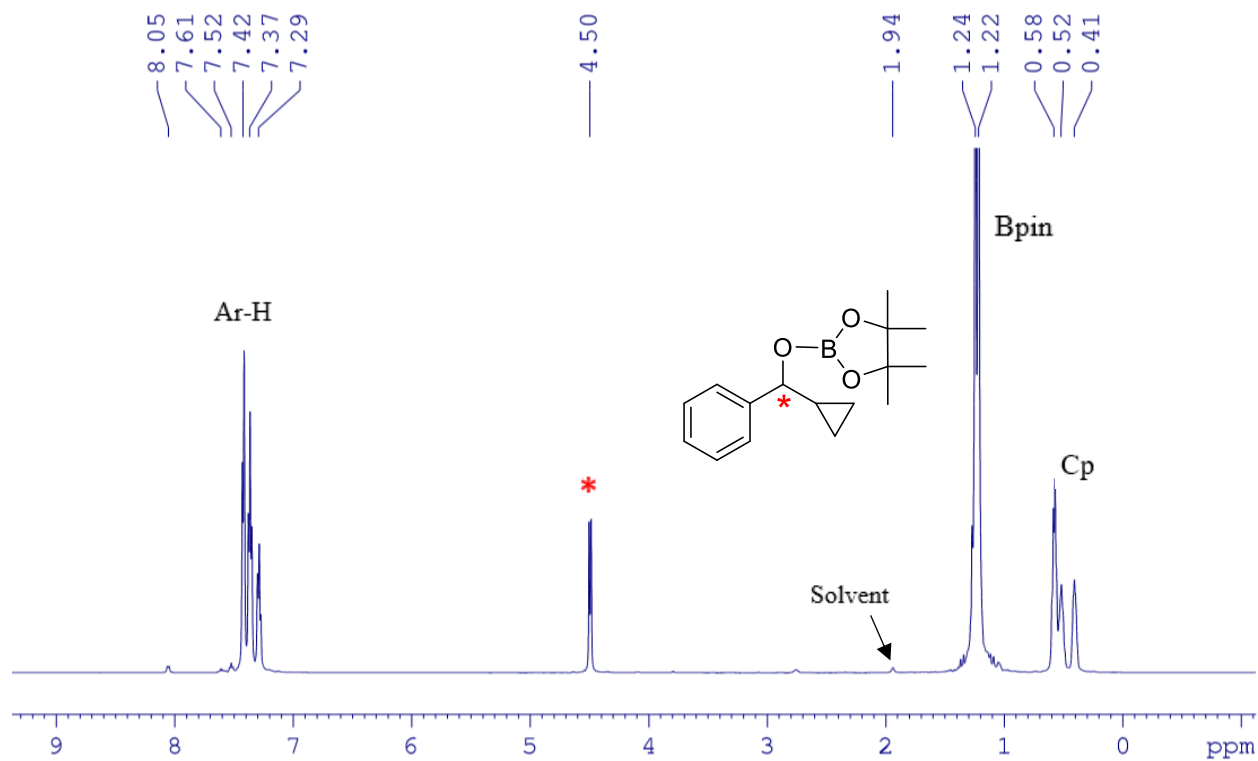


Figure S9. ¹H NMR spectra of reaction between Cyclopropylphenylketone and HBpin

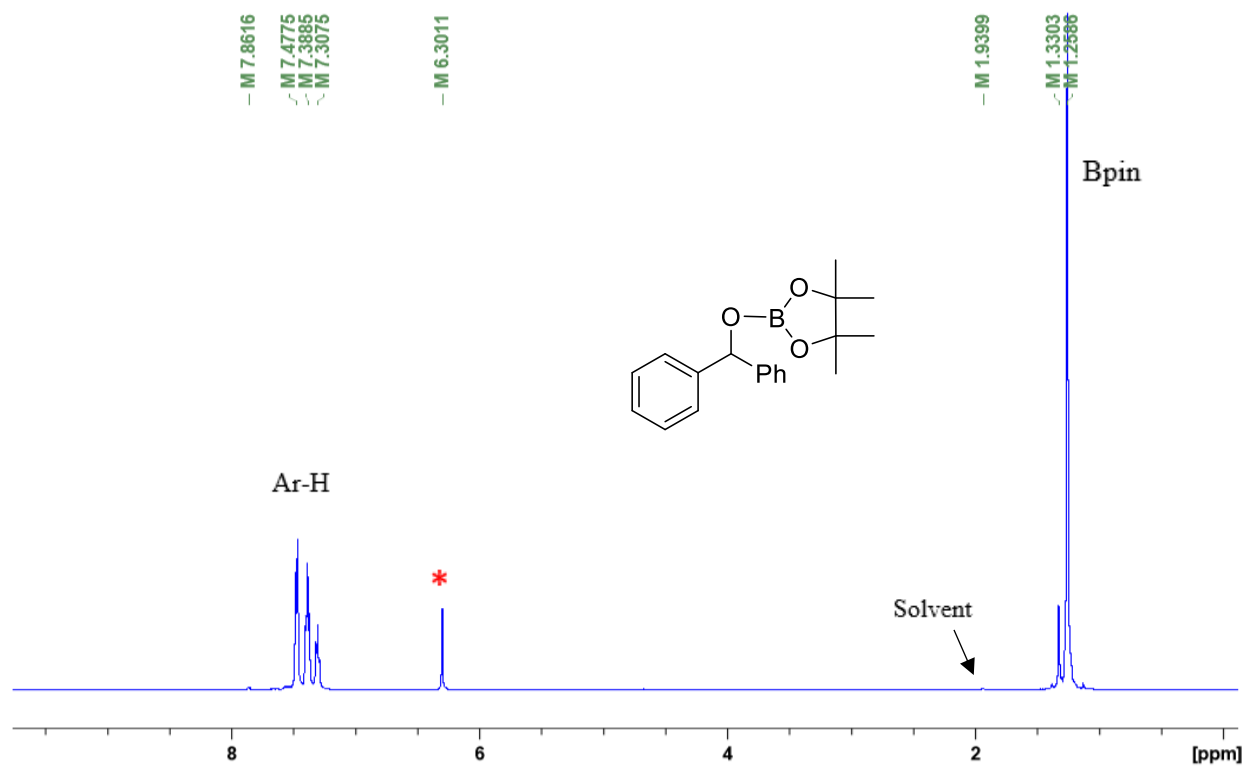


Figure S10. ¹H NMR spectra of reaction between Benzophenone and HBpin

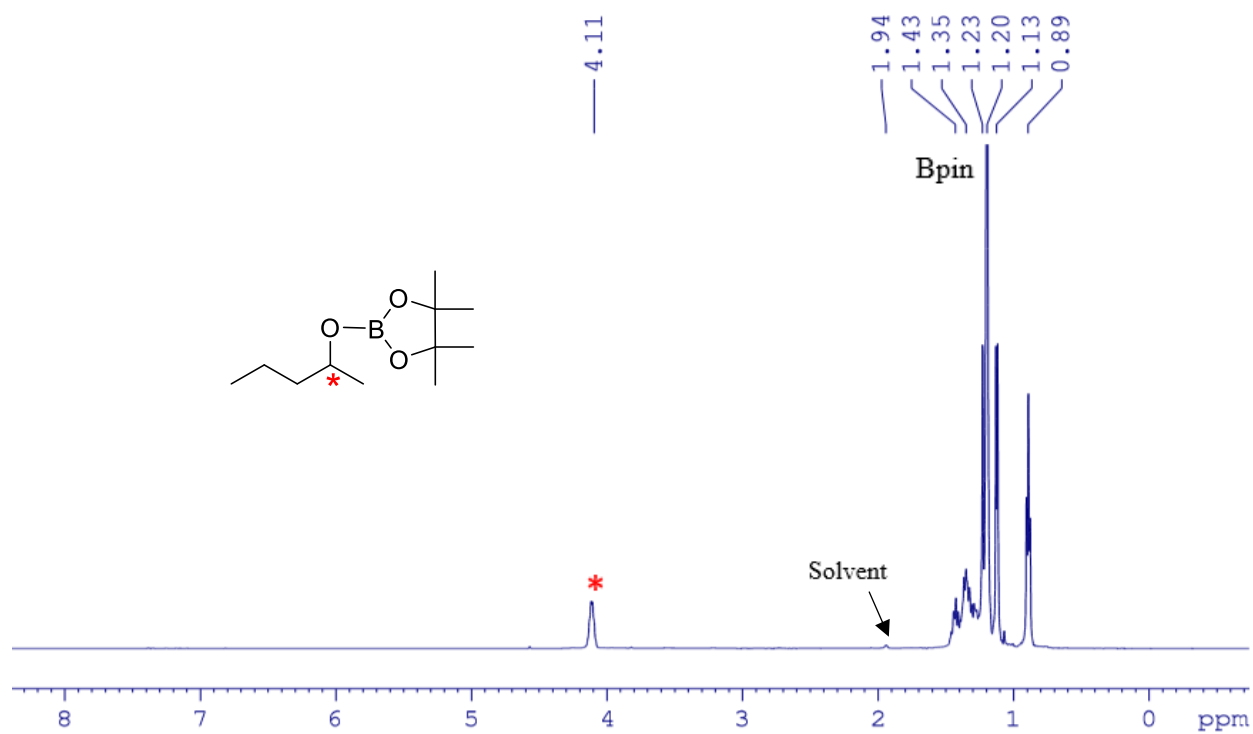


Figure S11. ^1H NMR spectra of reaction between 2-pentanone and HBpin

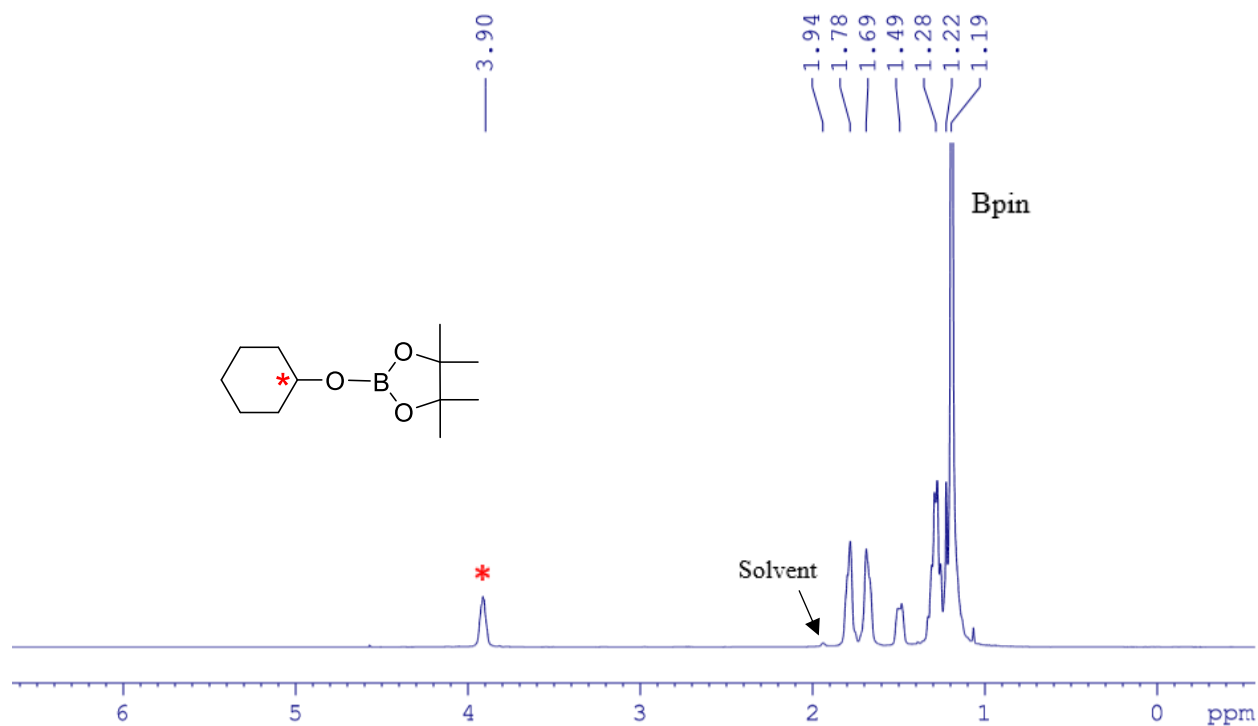


Figure S12. ^1H NMR spectra of reaction between Cyclohexanone and HBpin

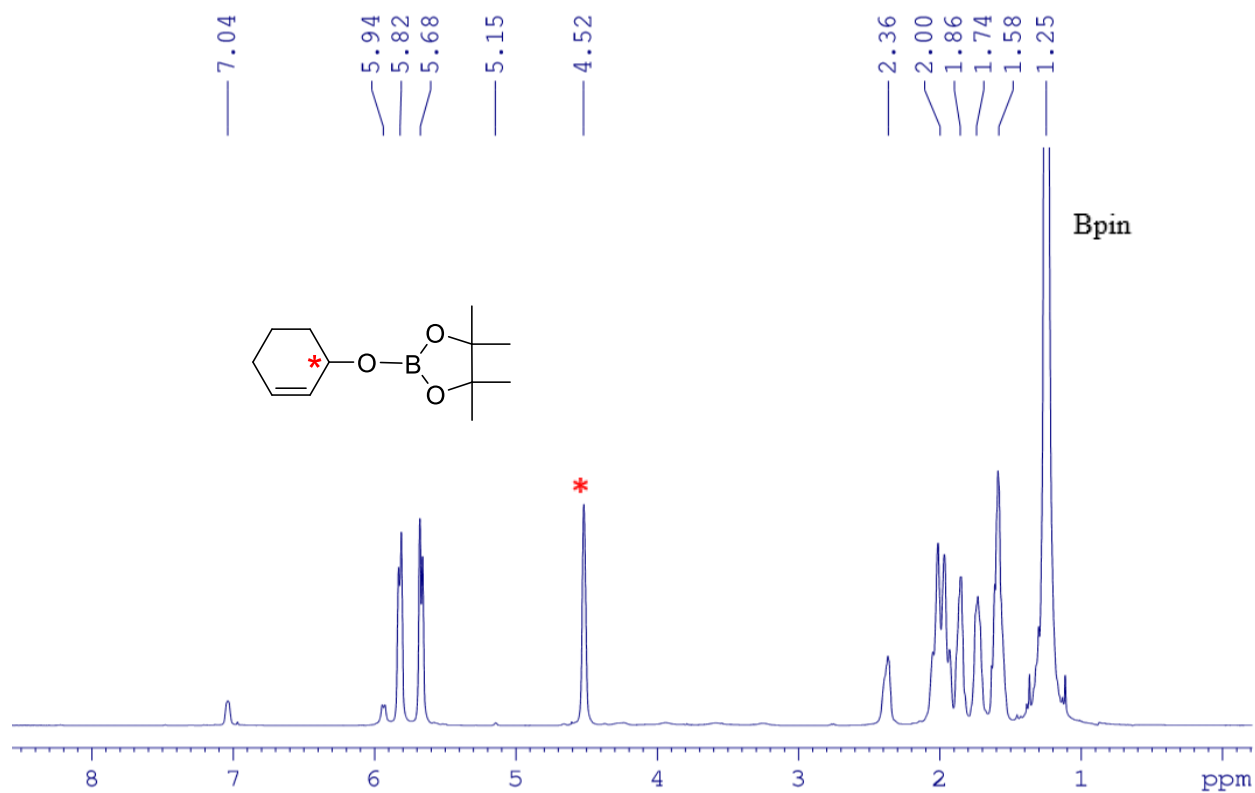


Figure S13. ^1H NMR spectra of reaction between 2-cyclohexenone and HBpin

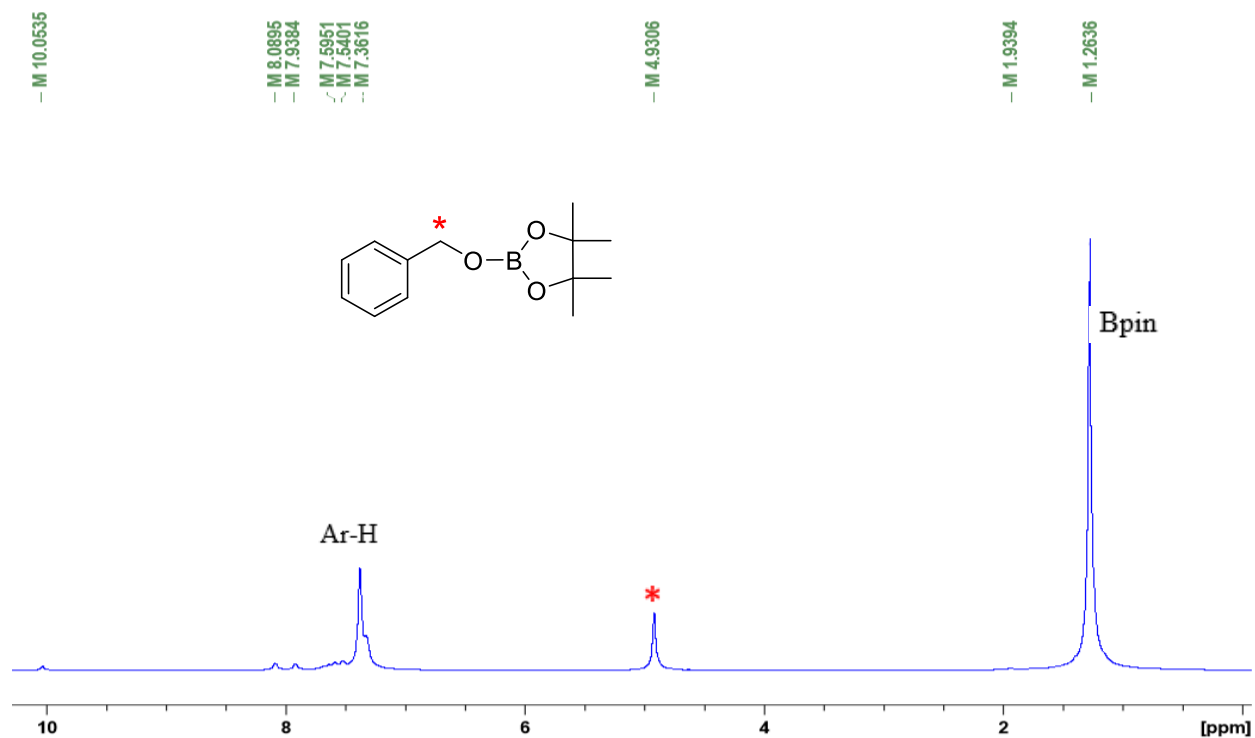


Figure S14. ^1H NMR spectra of reaction between PhCHO and HBpin

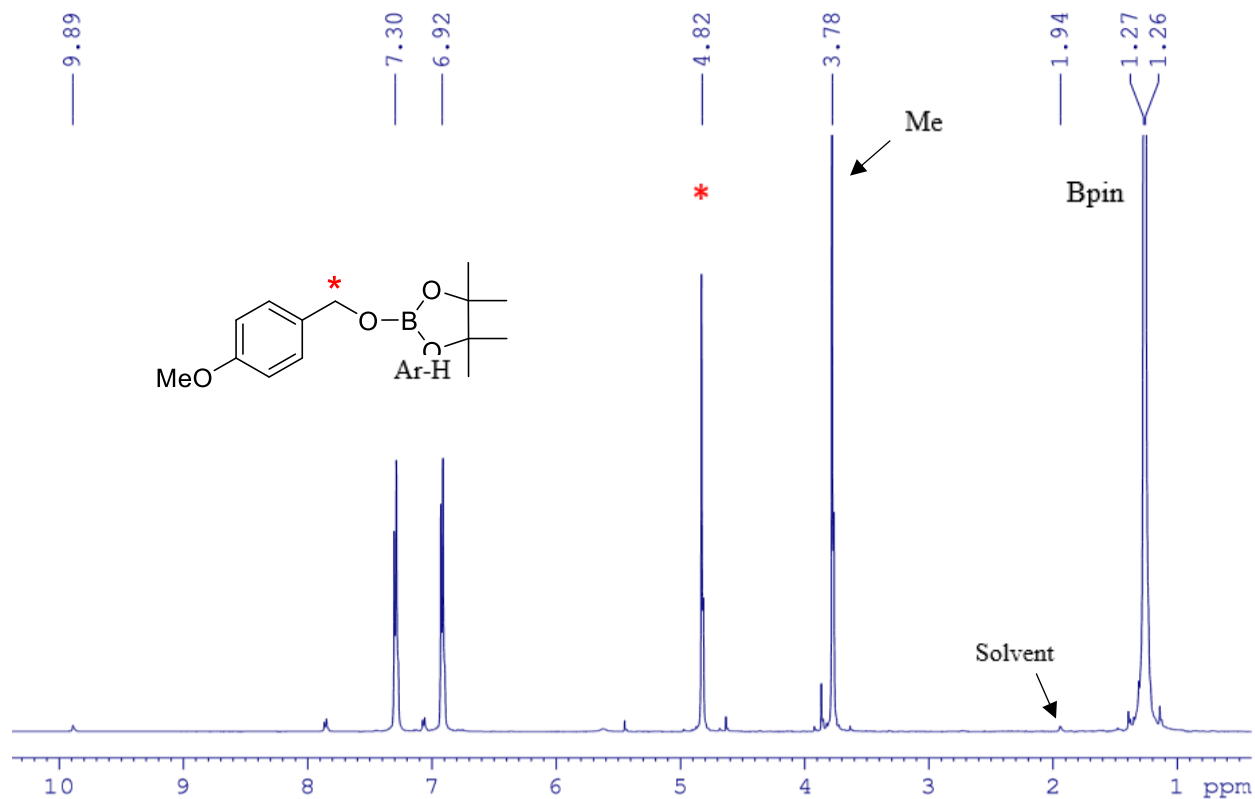


Figure S15. ¹H NMR spectra of reaction between *p*-MeO-PhCHO and HBpin

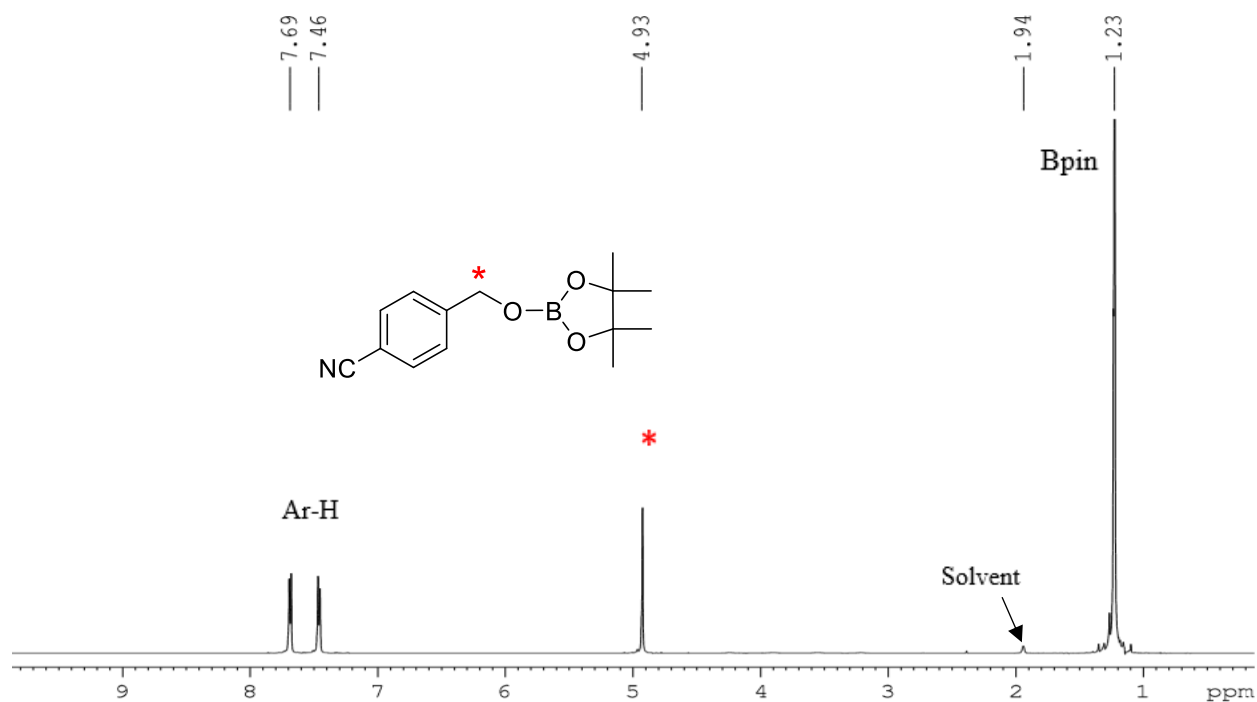


Figure S16. ¹H NMR spectra of reaction between *p*-CN-PhCHO and HBpin

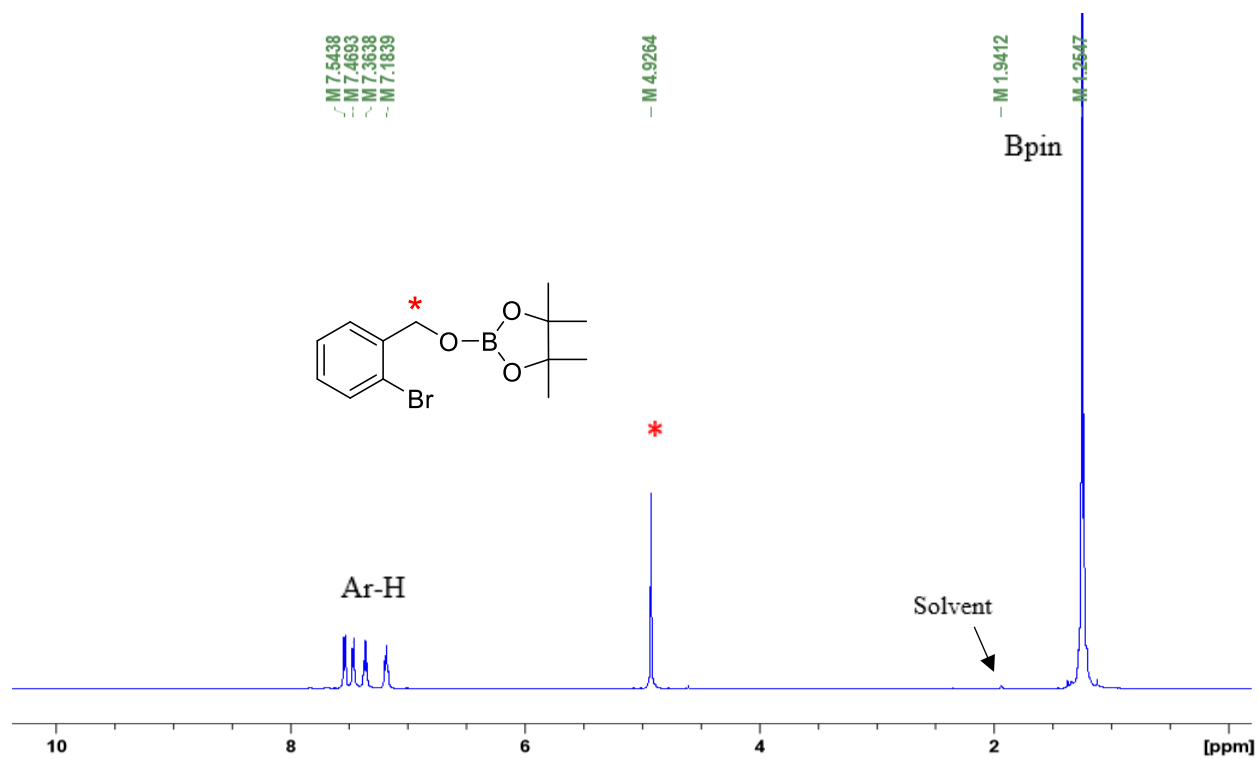


Figure S17. ^1H NMR spectra of reaction between *o*-Br-PhCHO and HBpin

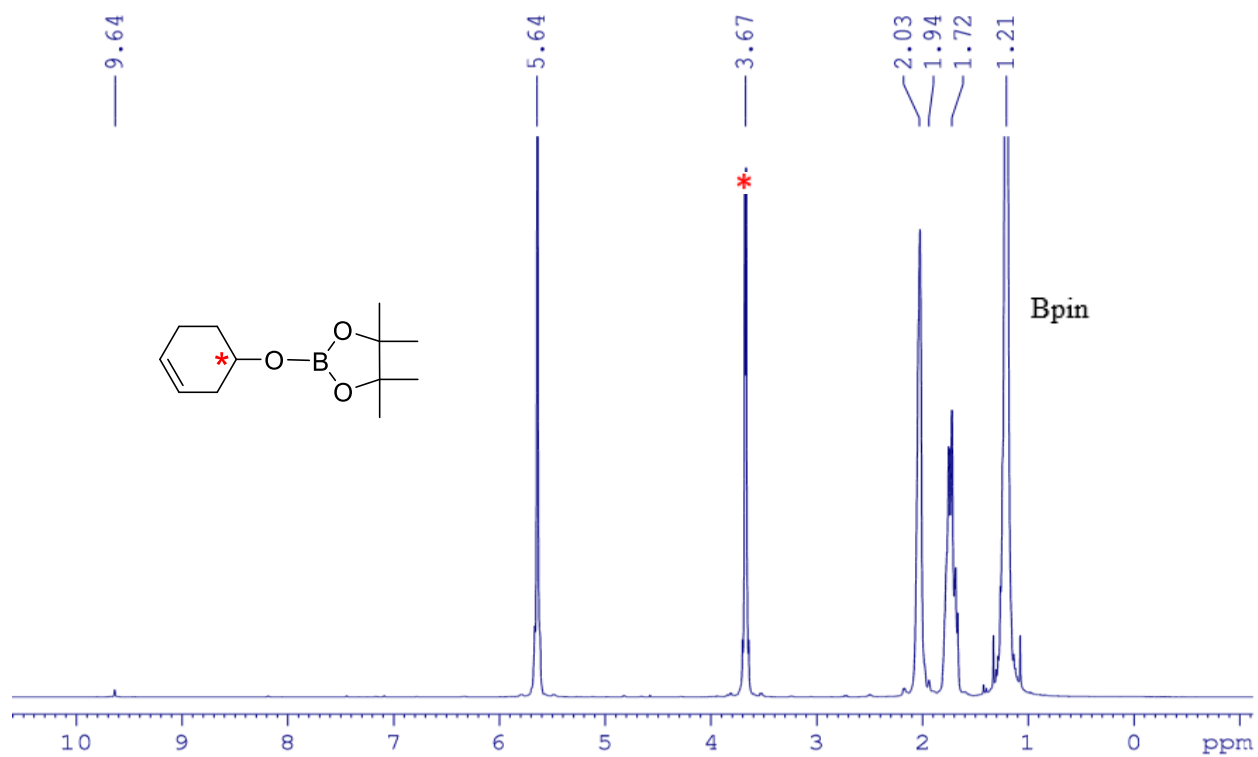


Figure S18. ^1H NMR spectra of reaction between cyclohexenecarboxaldehyde and HBpin

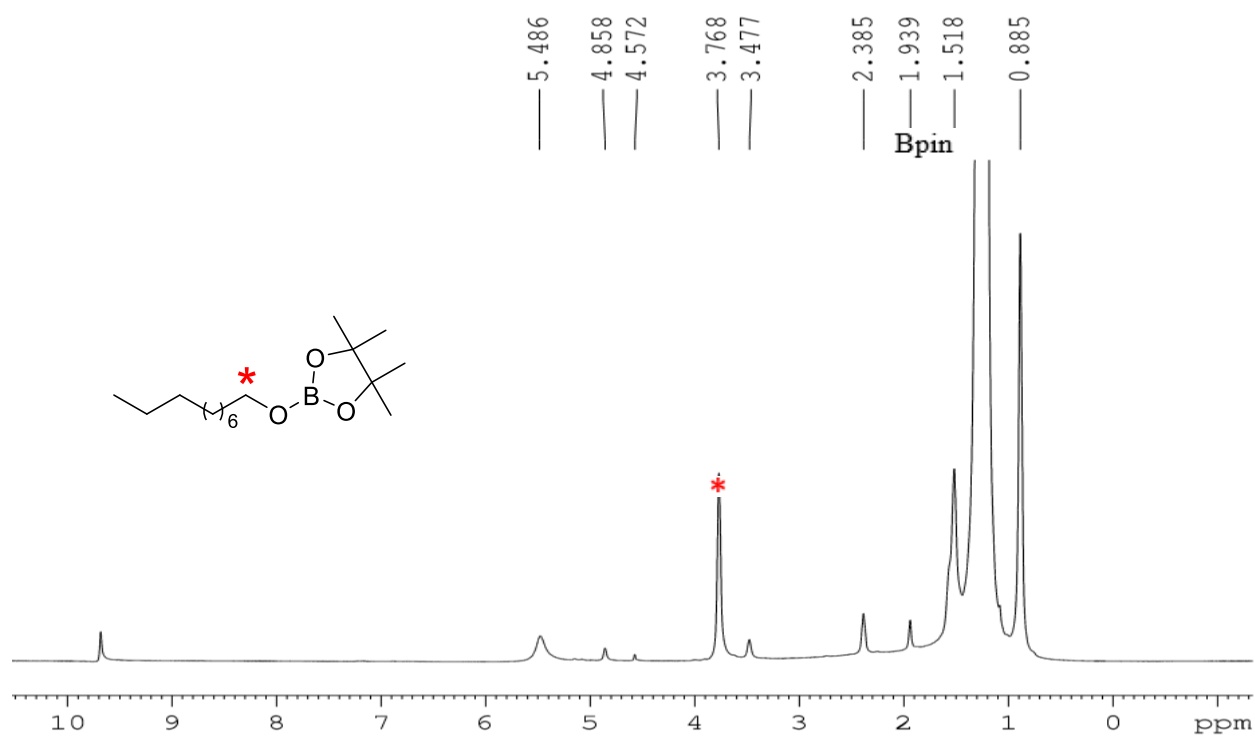


Figure S19. ^1H NMR spectra of reaction between Decanal and HBpin

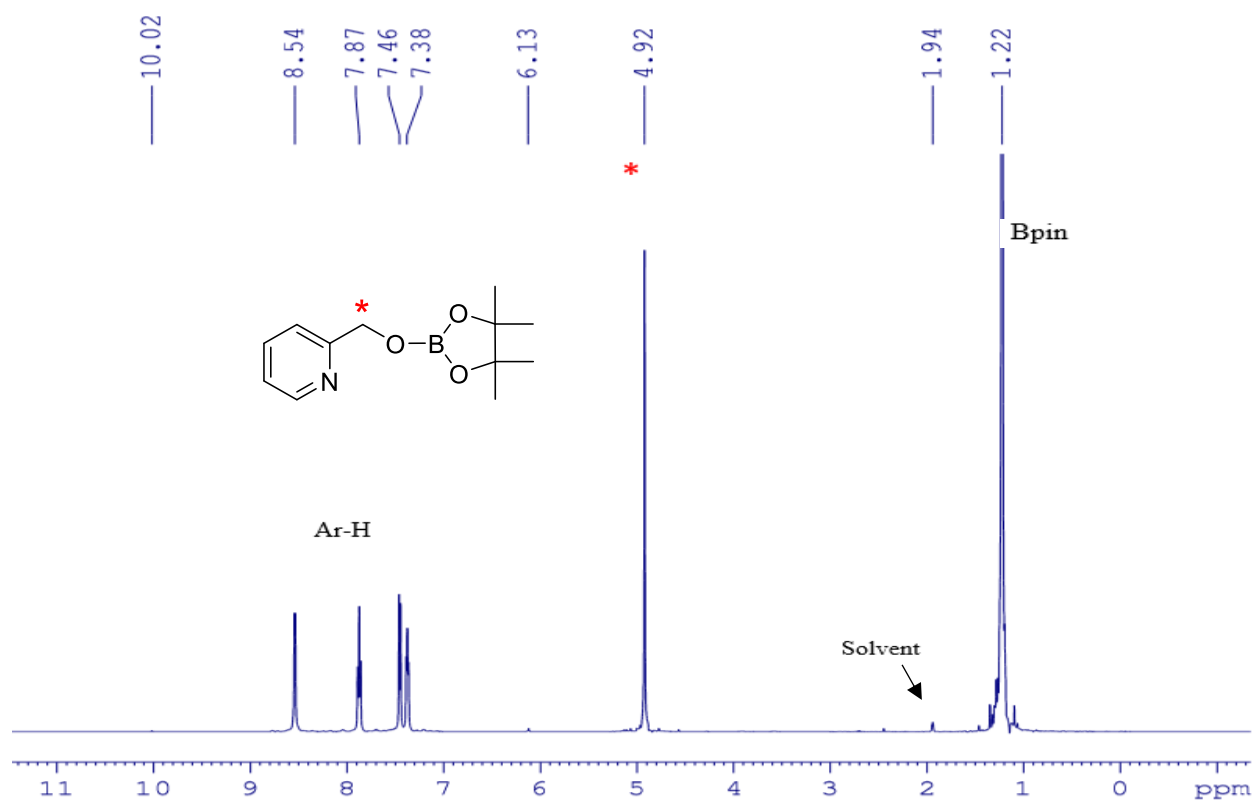


Figure S20. ^1H NMR spectra of reaction between 2-formylpyridine and HBpin

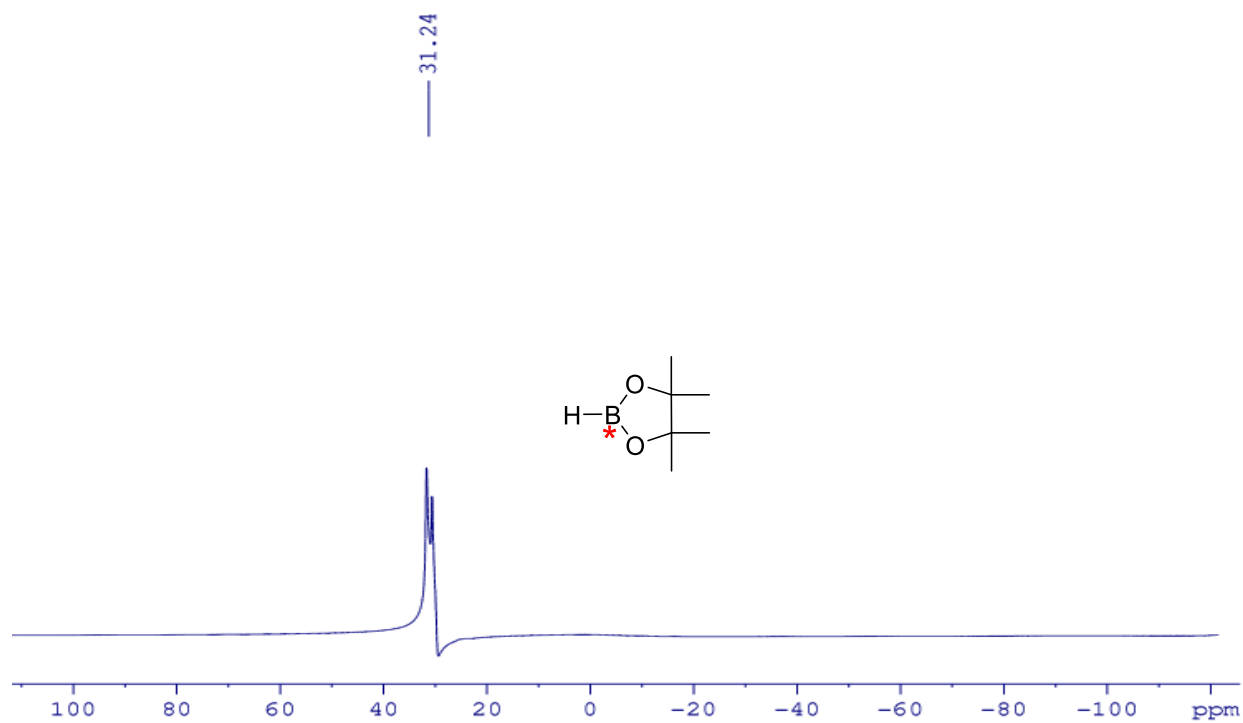


Figure S21. ^{11}B NMR spectra of HBpin

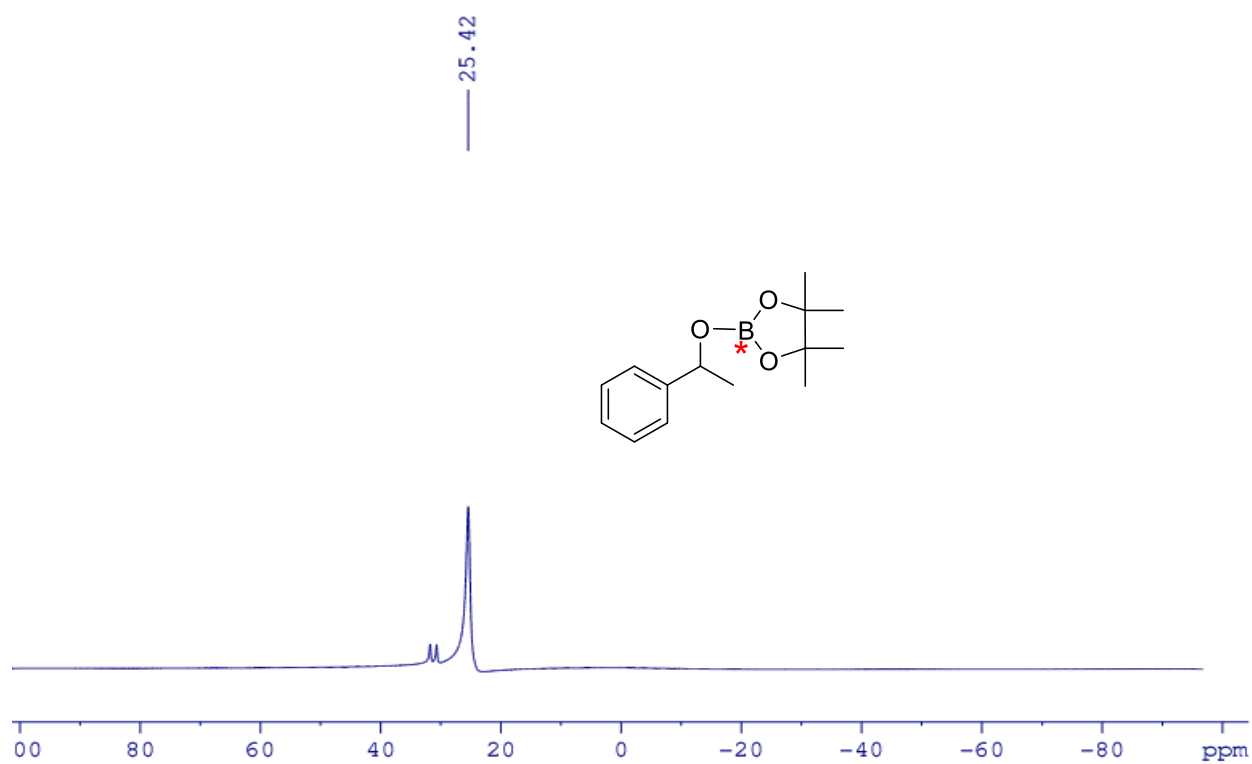


Figure S22. ^{11}B NMR spectra of reaction between AcPh and HBpin

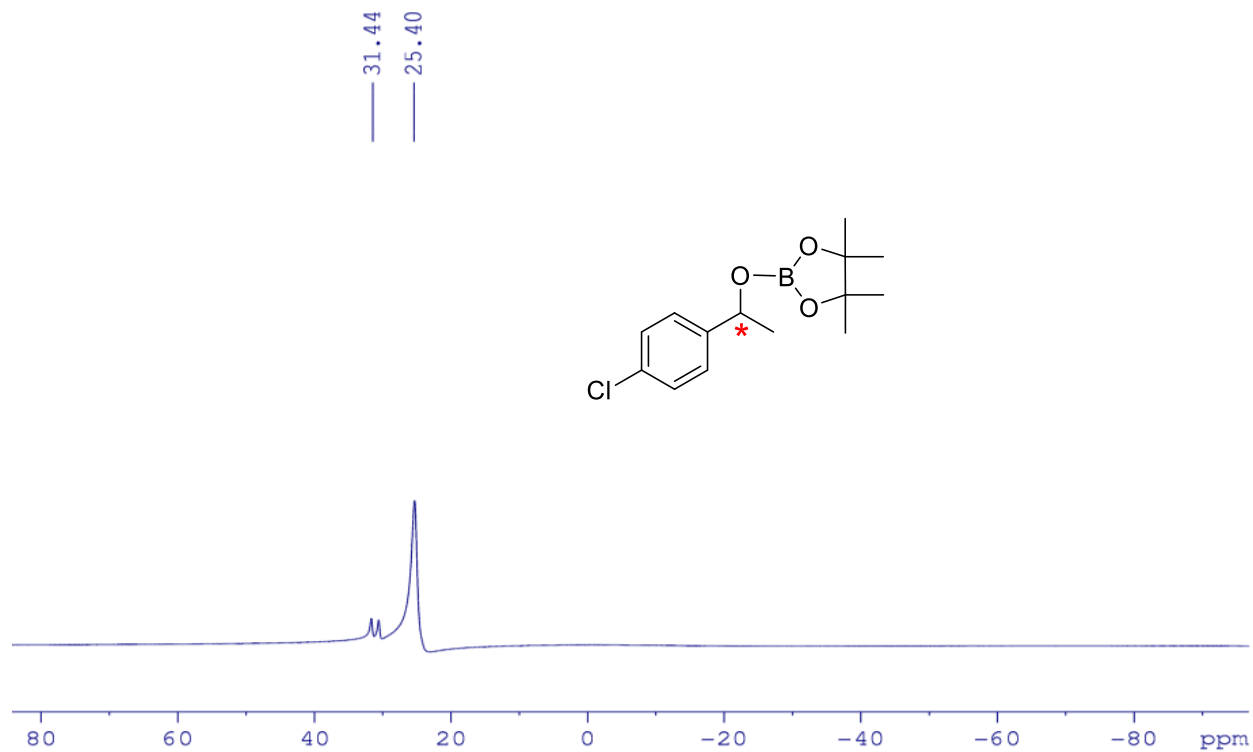


Figure S23. ¹¹B NMR spectra of reaction between *p*-Cl-AcPh and HBpin

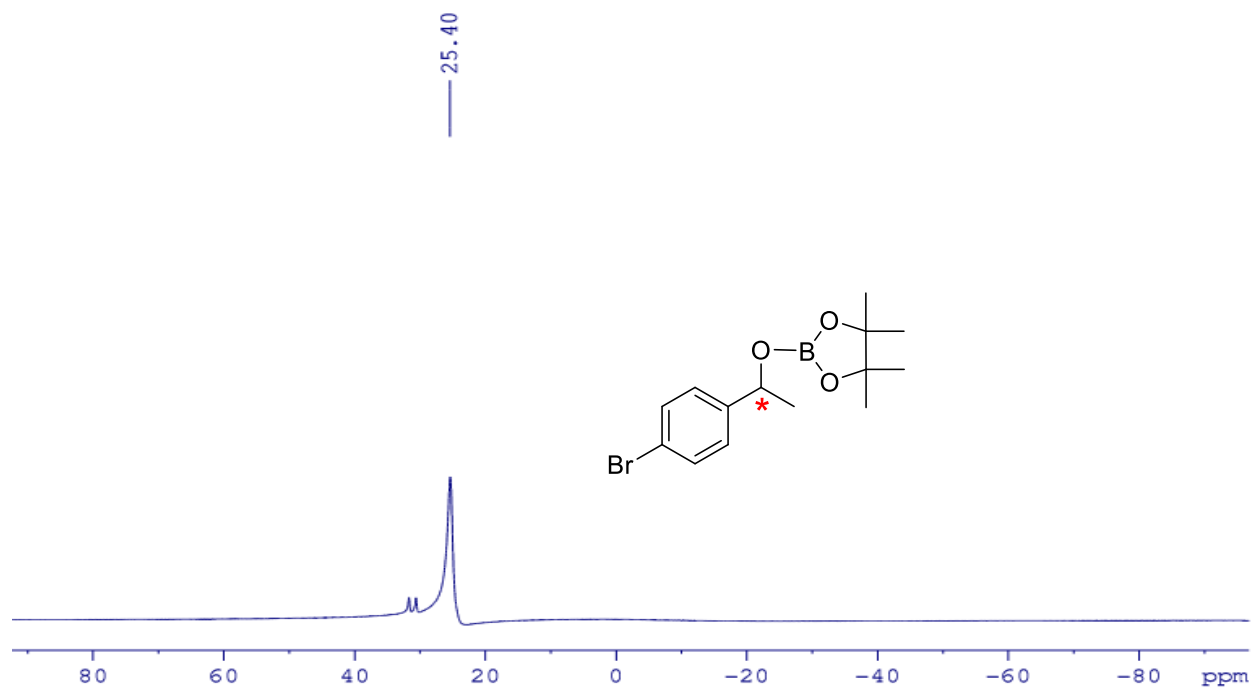
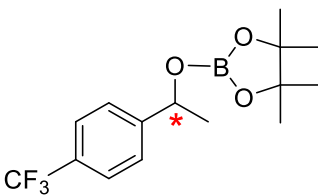
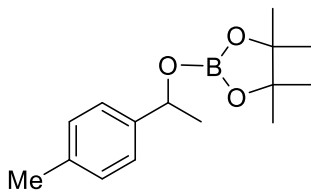


Figure S24. ¹¹B NMR spectra of reaction between *p*-Br-AcPh and HBpin



— 24.39



S23

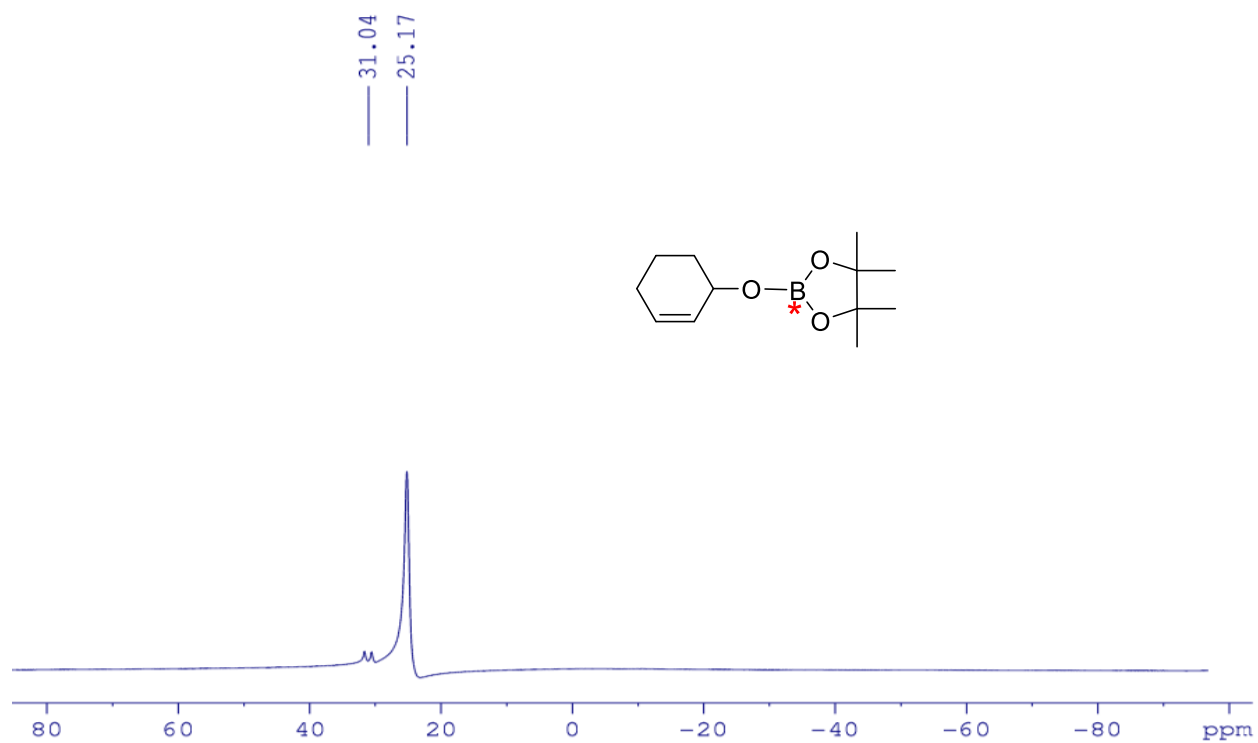


Figure S27. ^{11}B NMR spectra of reaction between 2-cyclohexenone and HBpin

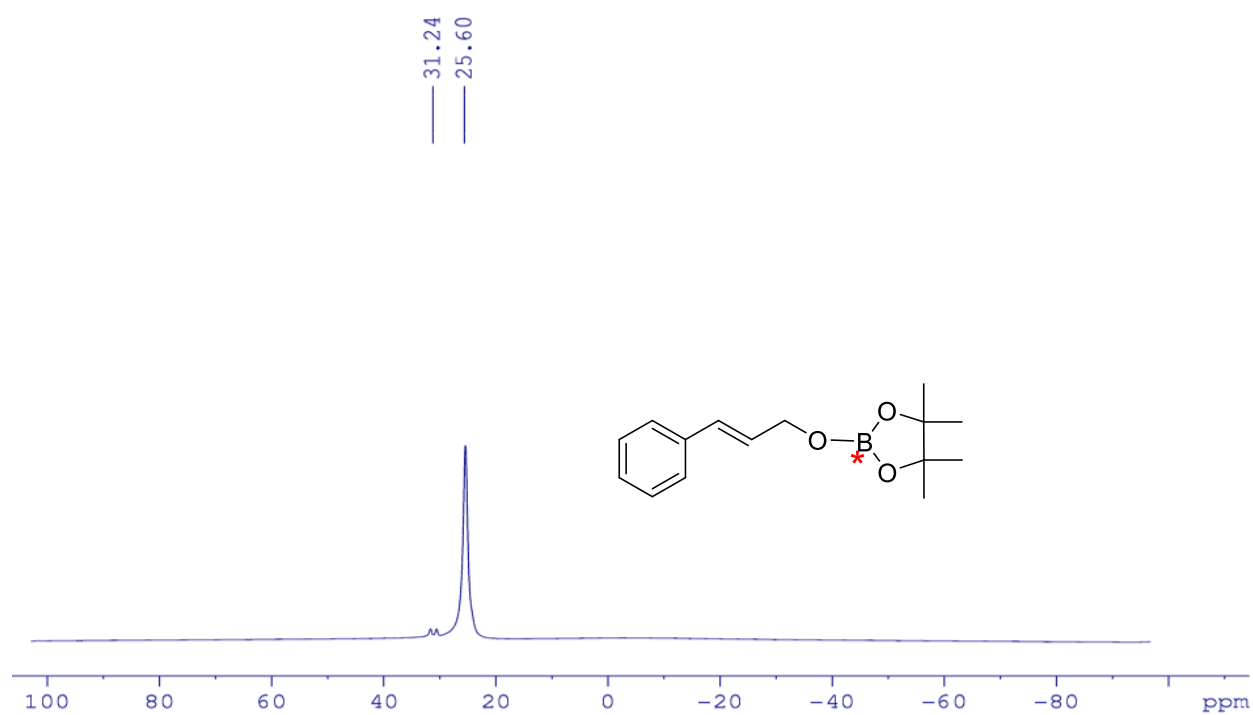


Figure S28. ^{11}B NMR spectra of reaction between *trans*-3-phenyl-2-propenal (cinnamaldehyde) and HBpin

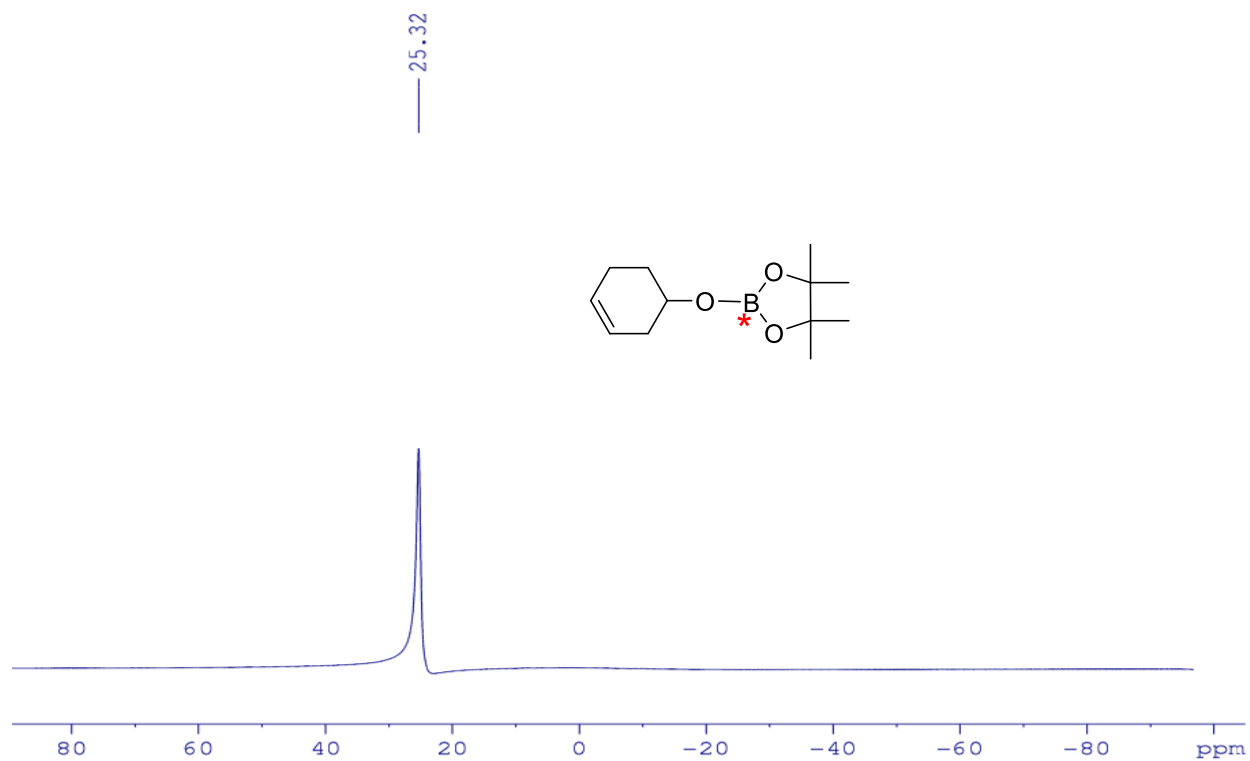


Figure S29. ^{11}B NMR spectra of reaction between Cyclohexenecarboxaldehyde and HBpin

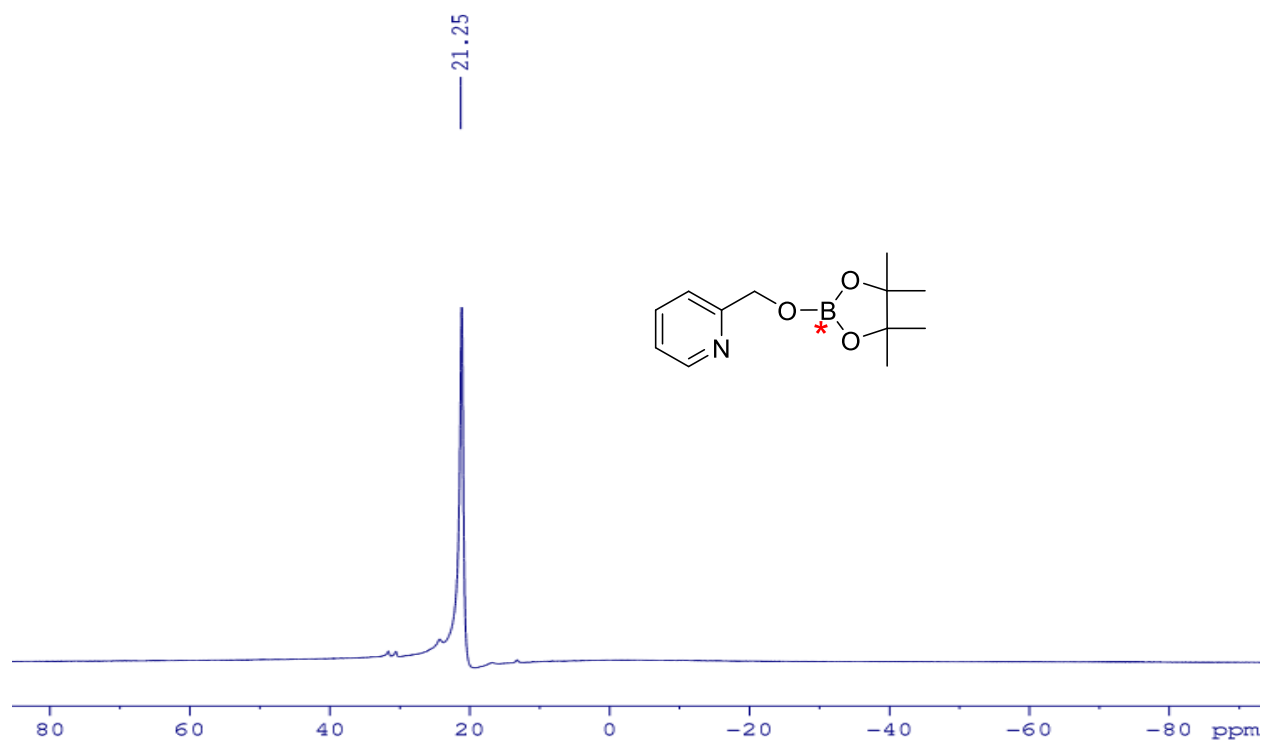


Figure S30. ^{11}B NMR spectra of reaction between 2-formylpyridine and HBpin

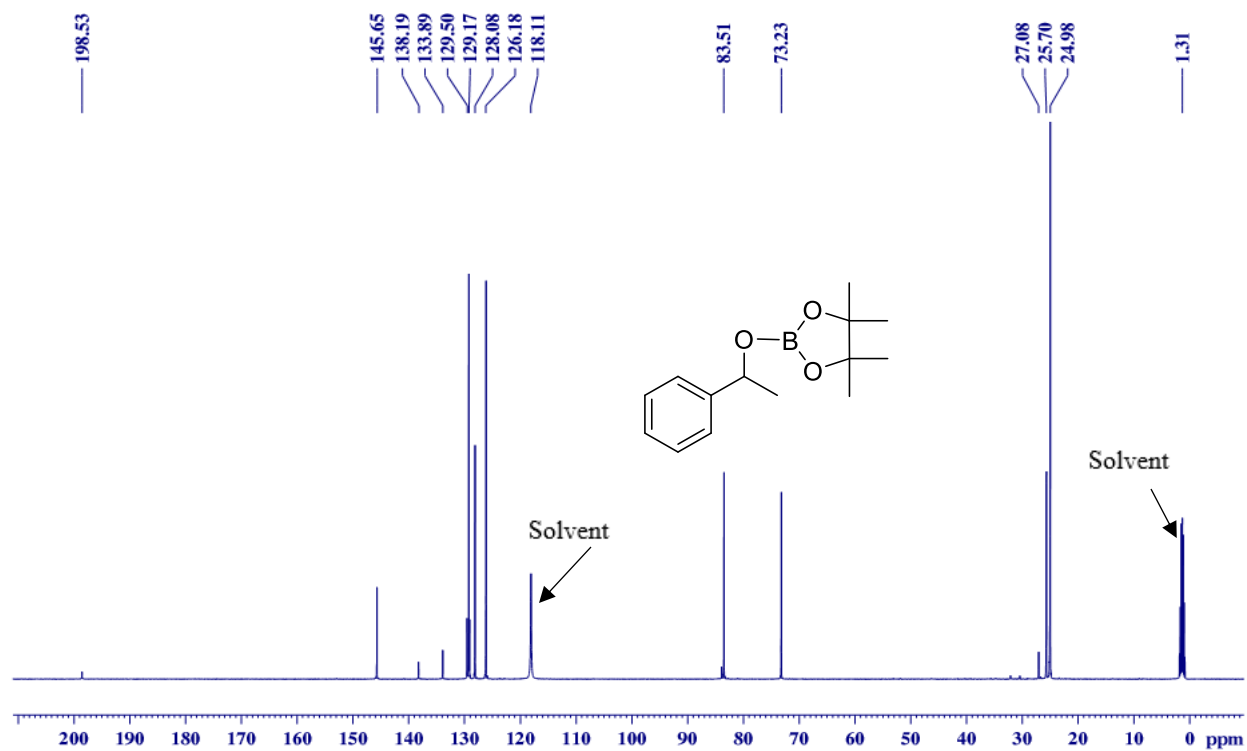


Figure S31. ¹³C NMR spectra of reaction between AcPh and HBpin

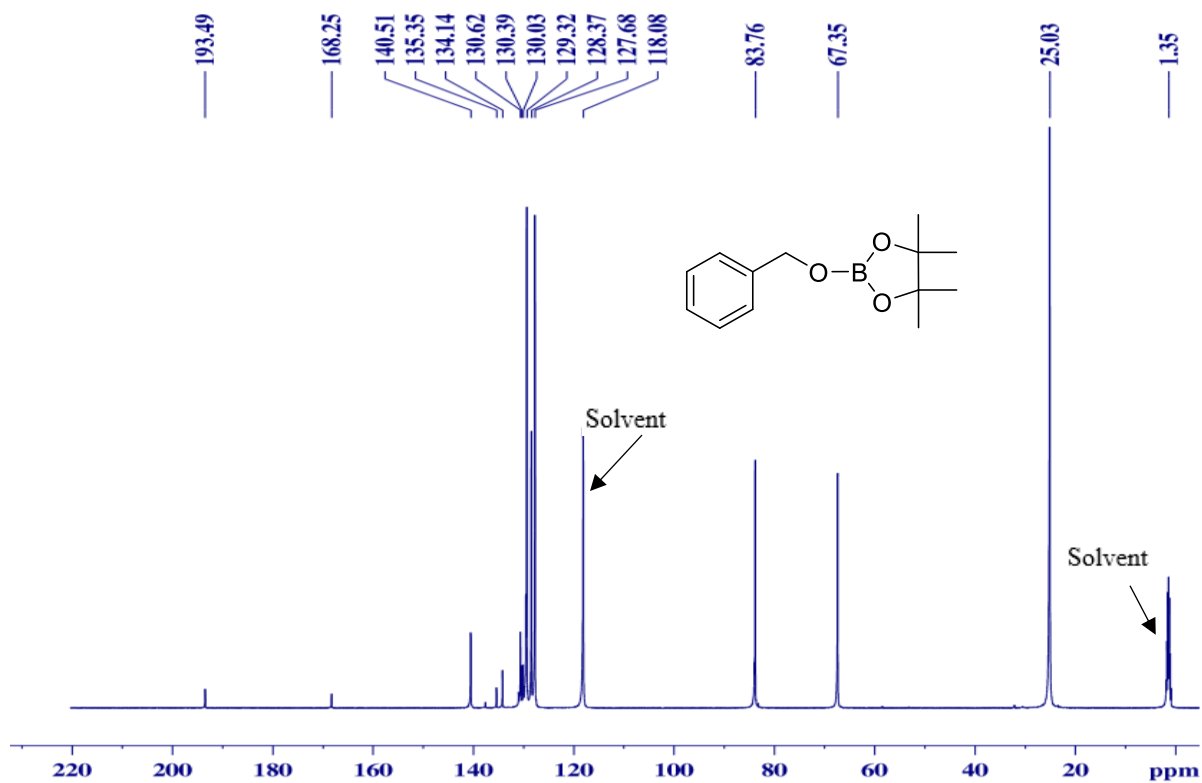


Figure S32. ¹³C NMR spectra of reaction between PhCHO and HBpin

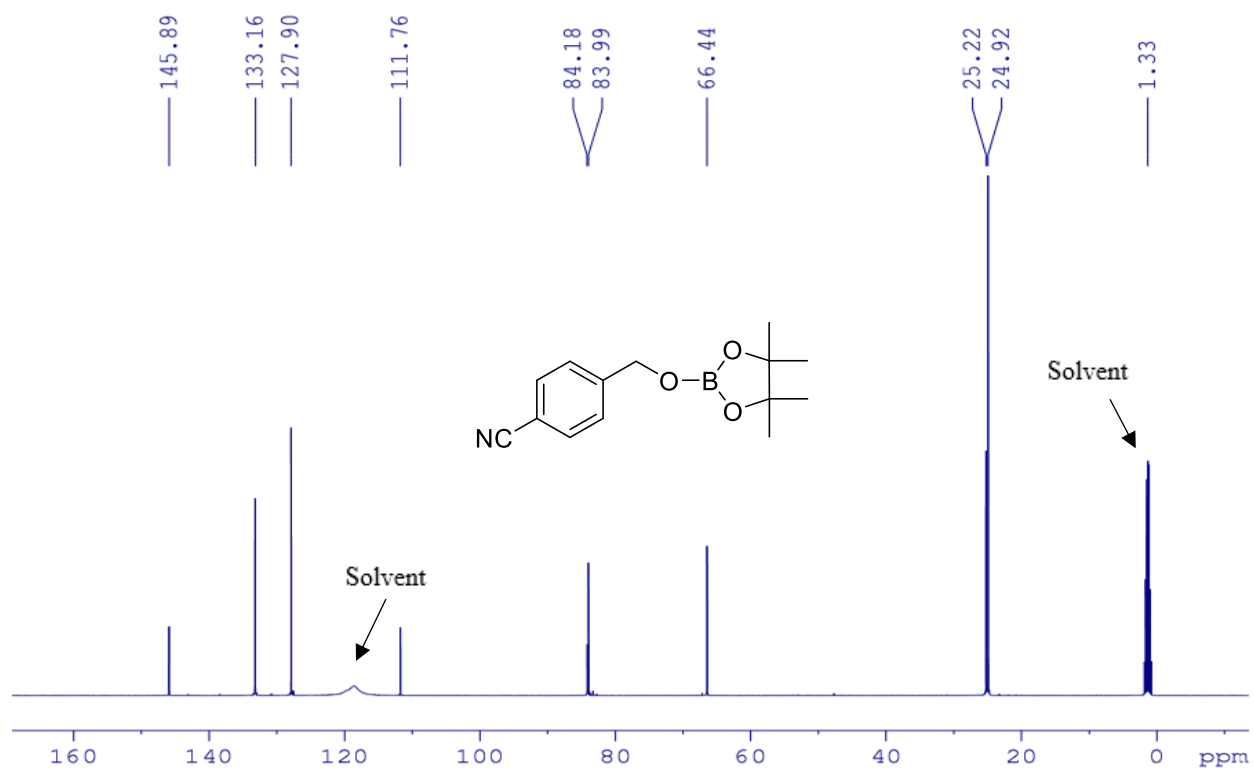


Figure S33. ¹³C NMR spectra of reaction between *p*-CN-PhCHO and HBpin

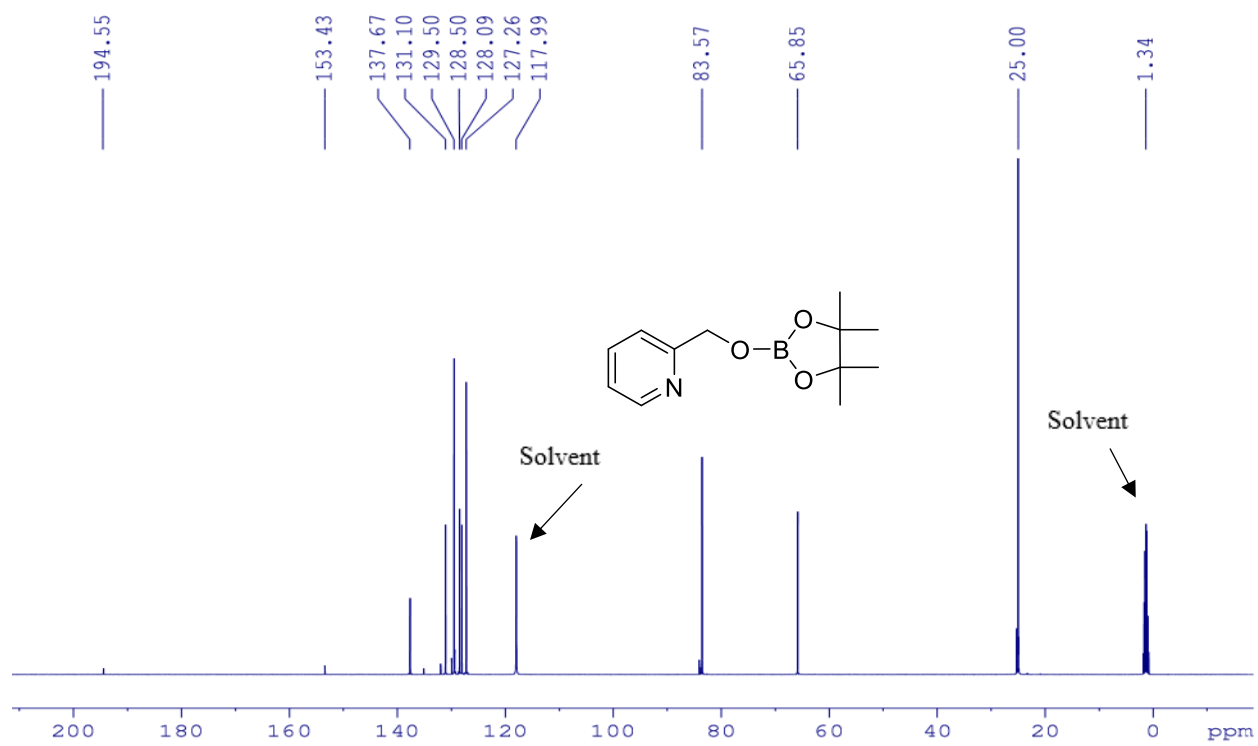


Figure S34. ^{13}C NMR spectra of reaction between 2-formylpyridine and HBpin

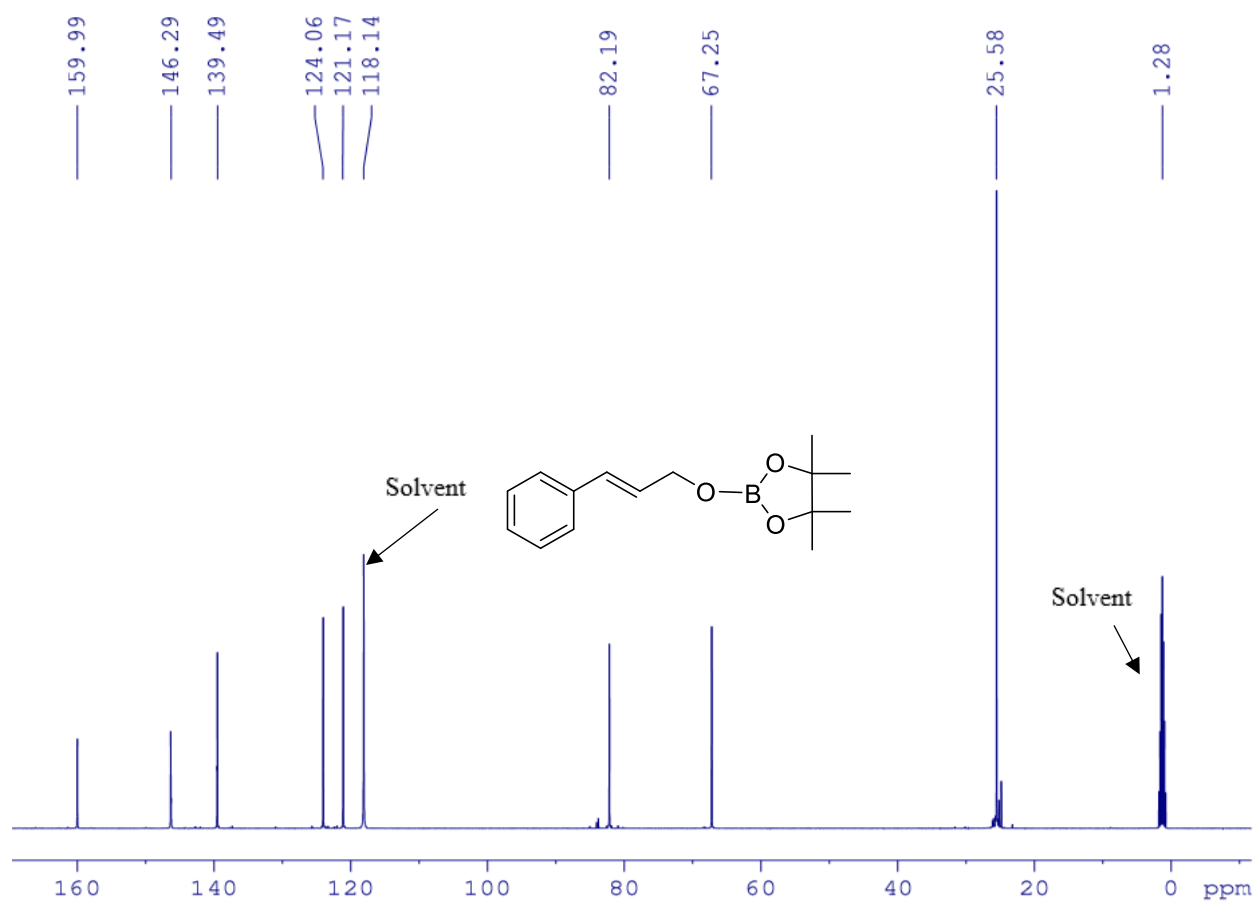


Figure S35. ^{13}C NMR spectra of reaction between *trans*-3-phenyl-2-propenal (cinnamaldehyde) and HBpin

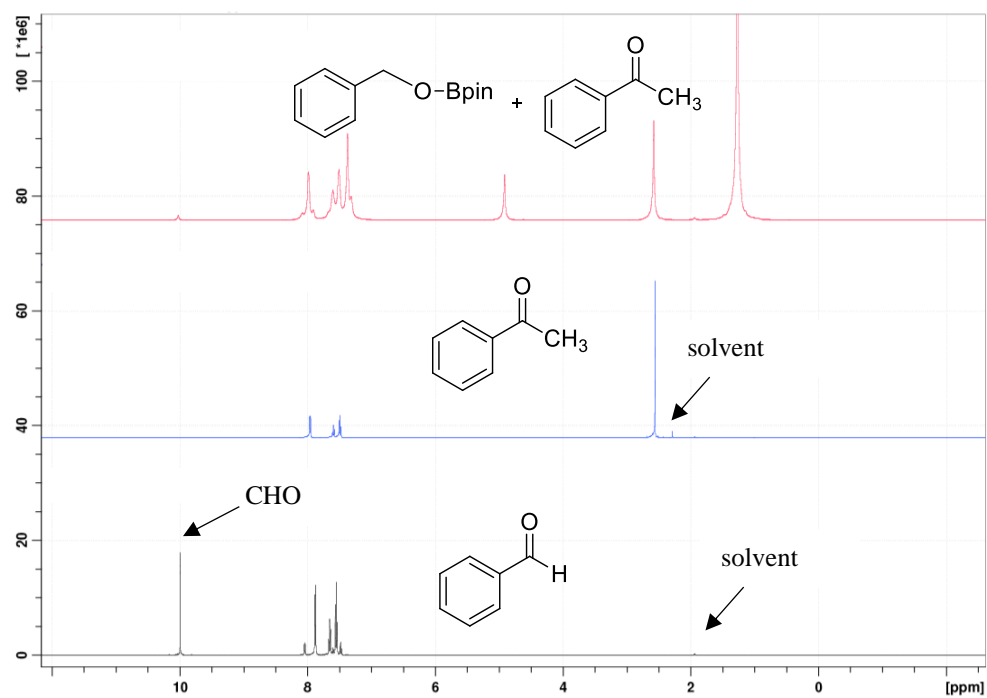


Figure S36. ^1H NMR spectra of intermolecular competition between AcPh and PhCHO with HBpin

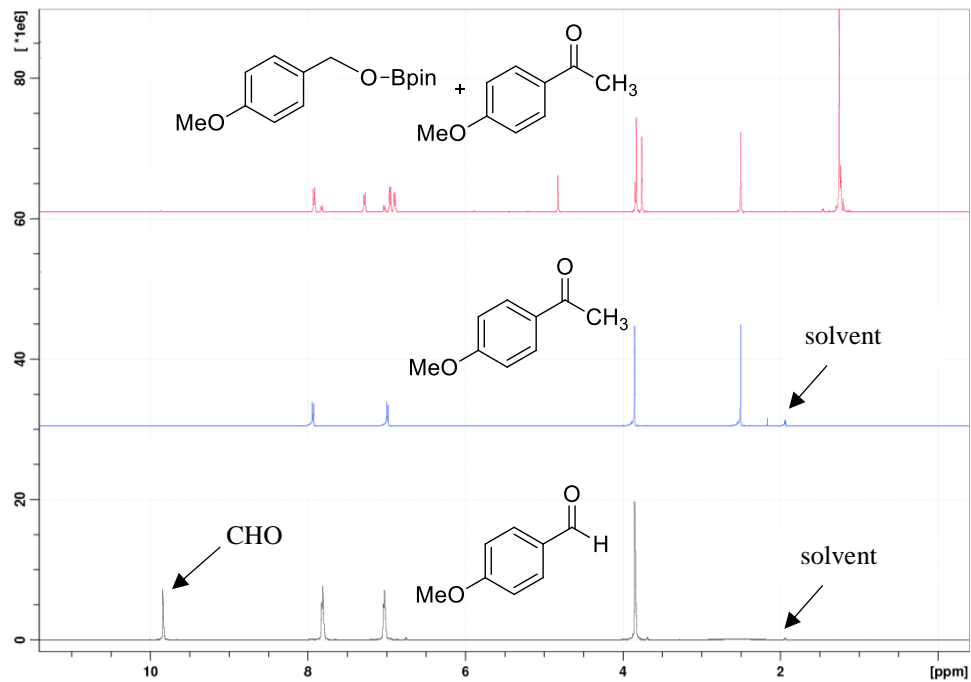


Figure S37. ^1H NMR spectra of intermolecular competition between *p*-MeO-AcPh and *p*-MeO-PhCHO with HBpin

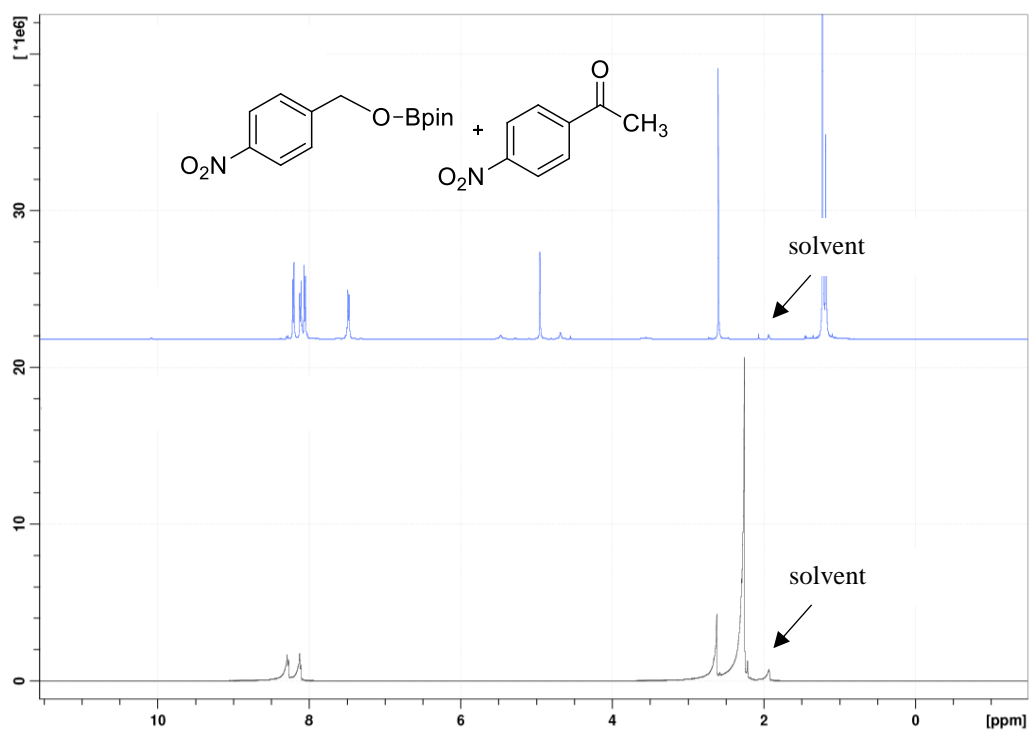


Figure S38. ^1H NMR spectra of intermolecular competition between $p\text{-NO}_2\text{-AcPh}$ and $p\text{-NO}_2\text{-PhCHO}$ with HBpin

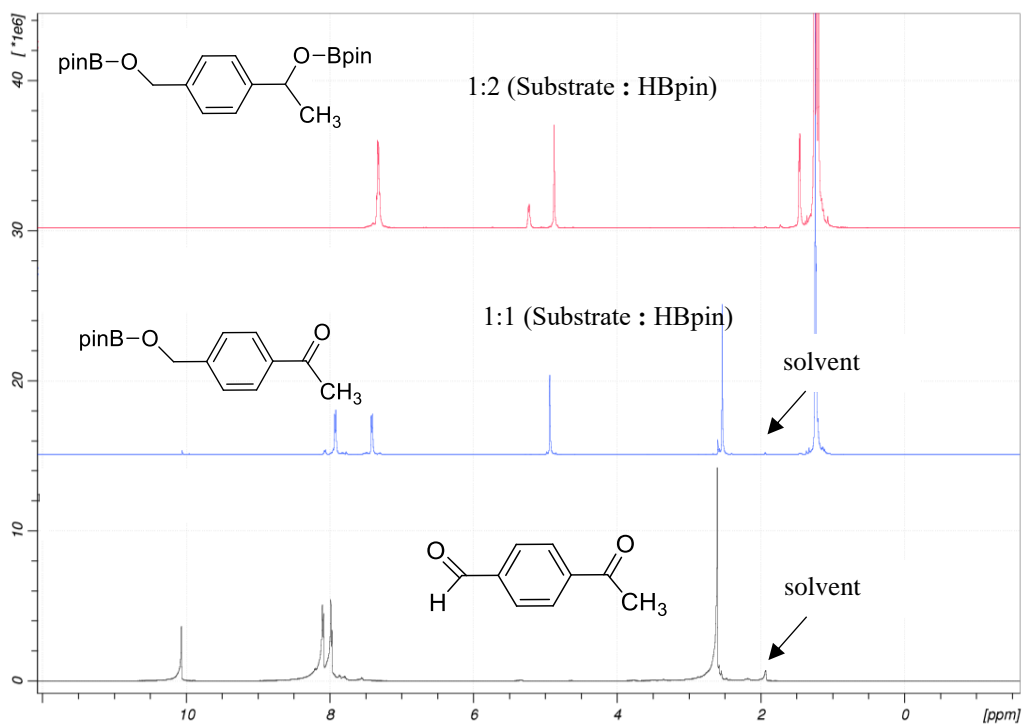


Figure S39. ^1H NMR spectra of intramolecular chemoselective reaction of acetylbenzaldehyde with HBpin

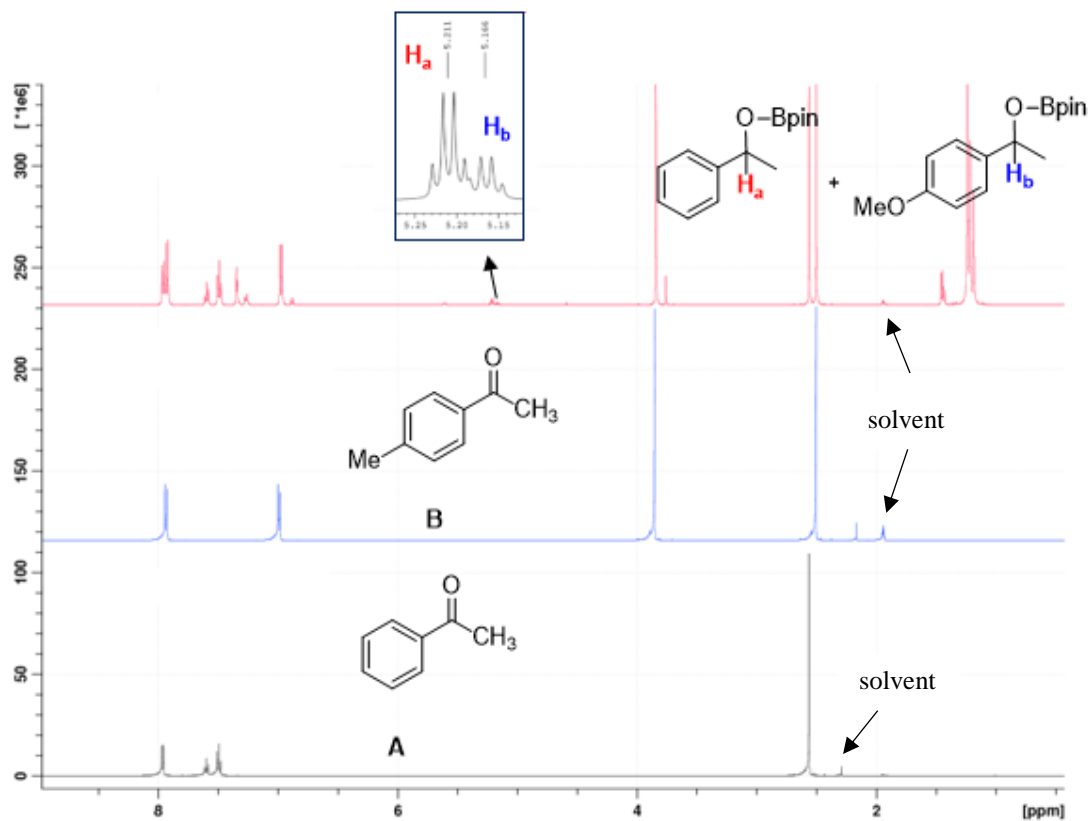


Figure S40. ^1H NMR spectra of competitive reaction between AcPh and p -CH₃O-AcPh with HBpin

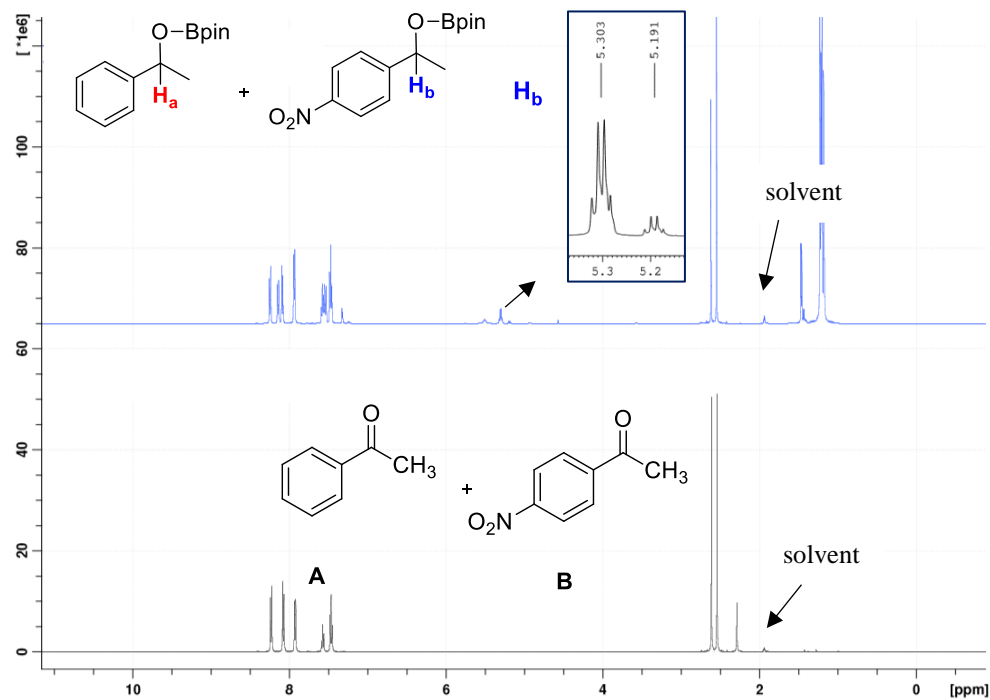


Figure S41. ^1H NMR spectra of competition reaction between AcPh and p -NO₂-AcPh with HBpin

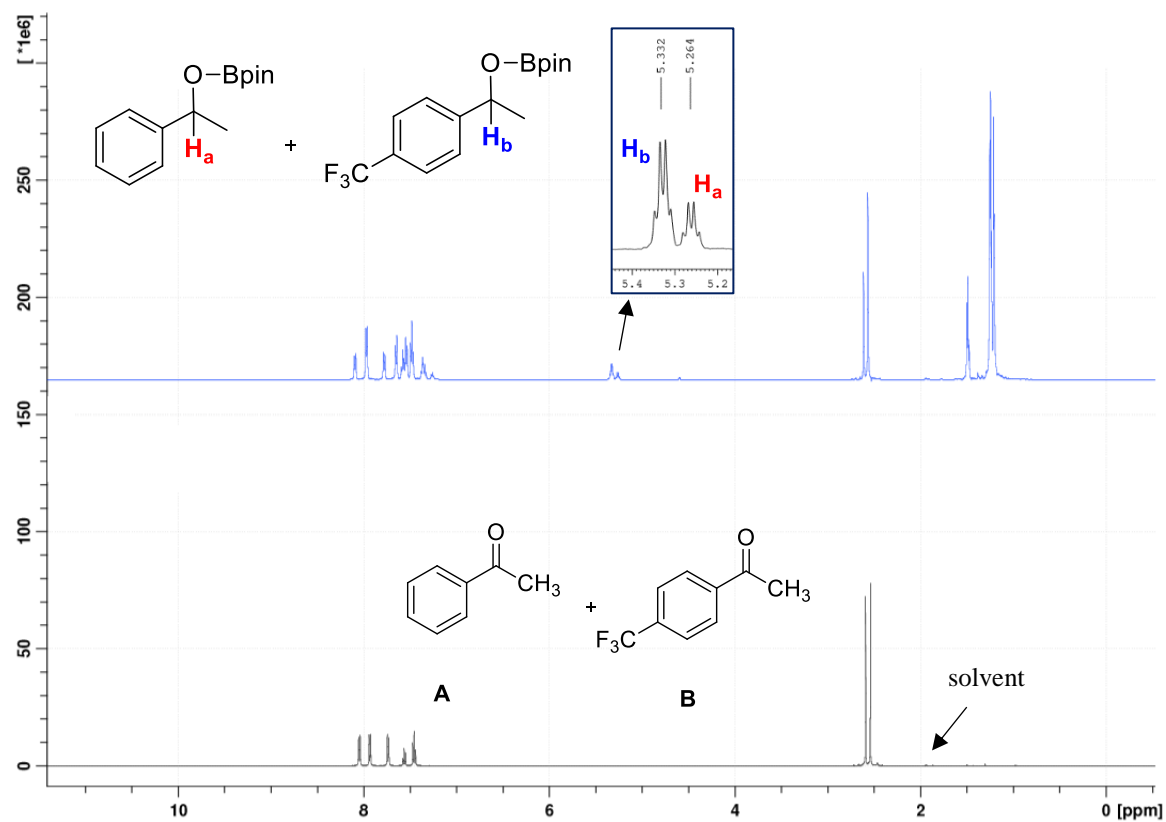


Figure S42. ^1H NMR spectra of competition reaction between AcPh and $p\text{-CF}_3\text{-AcPh}$ with HBpin

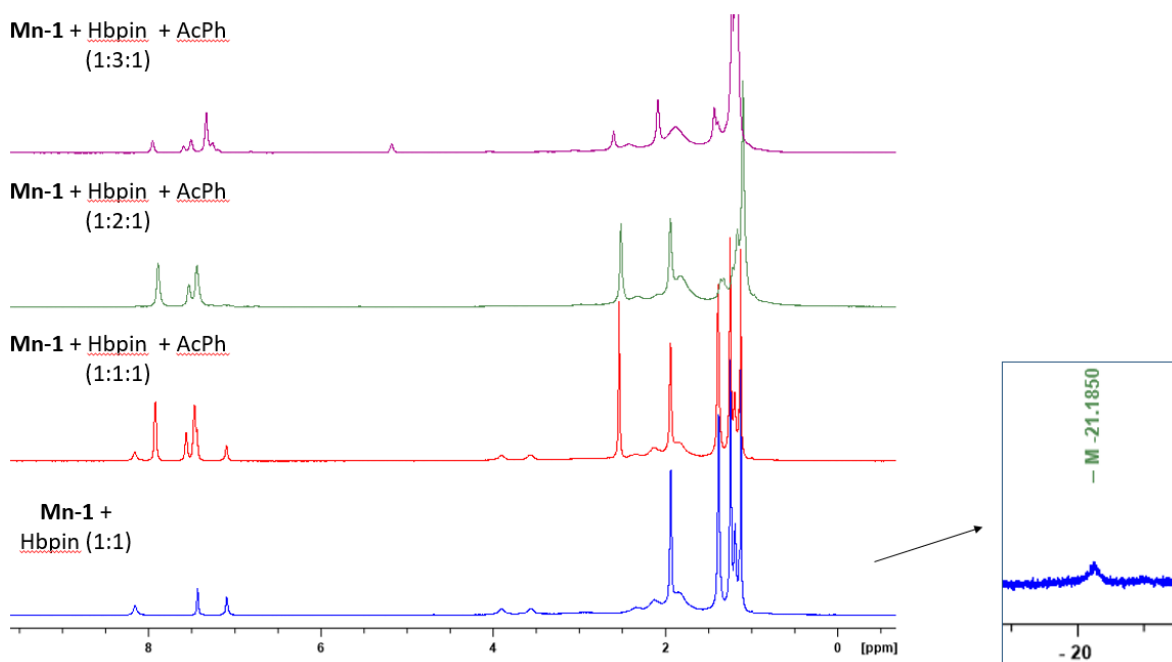
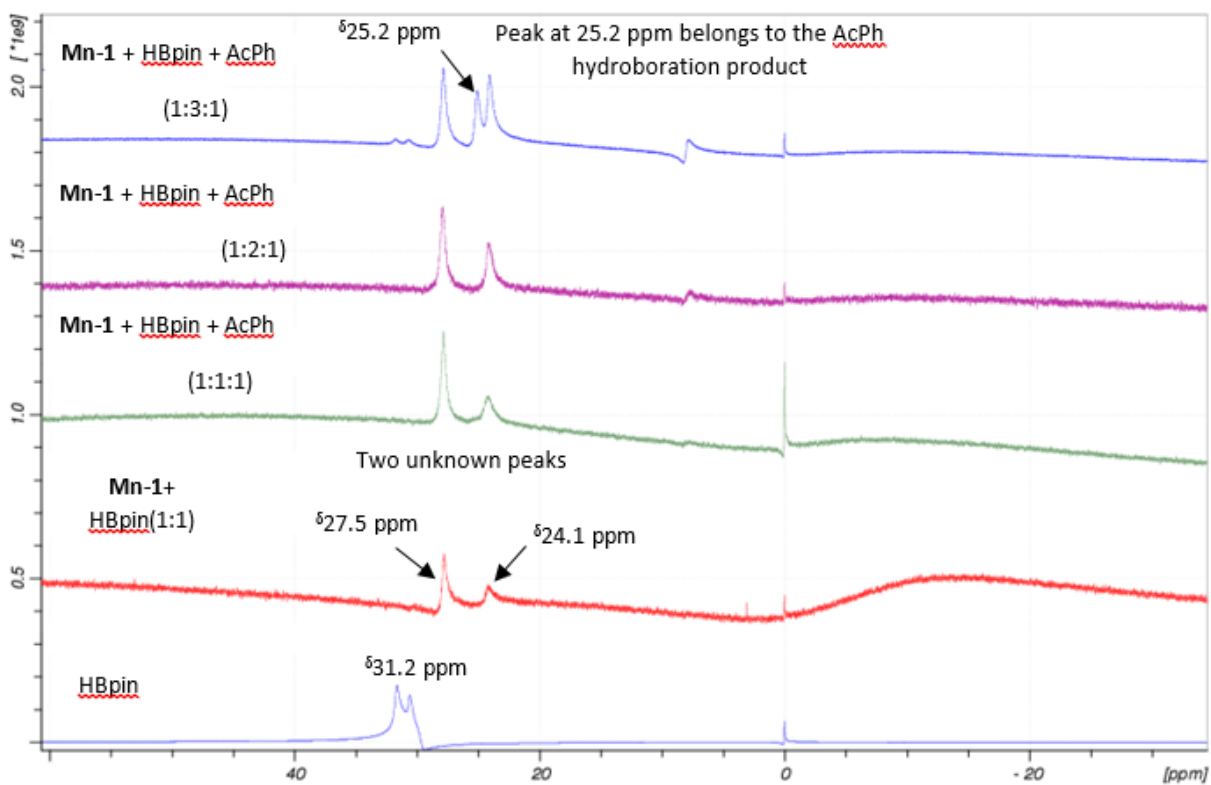


Figure S43. ^{11}B (top) and ^1H (bottom) NMR of catalyst (**Mn-1**) with HBpin and AcPh

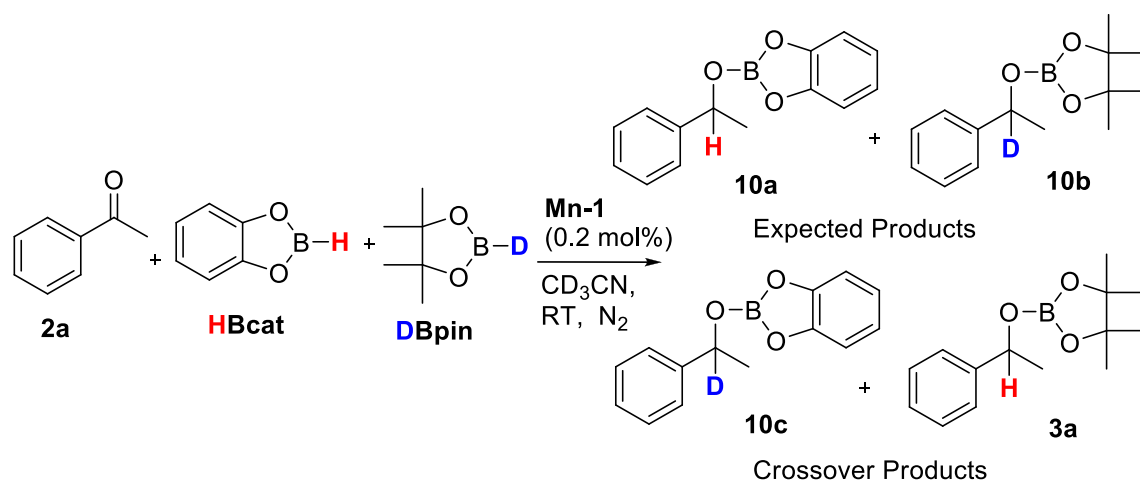


Figure S44. Reaction scheme of HBcat and DBpin with acetophenone

(**10a** and **10b** are the expected products; **10c** and **3a** are the crossover products)

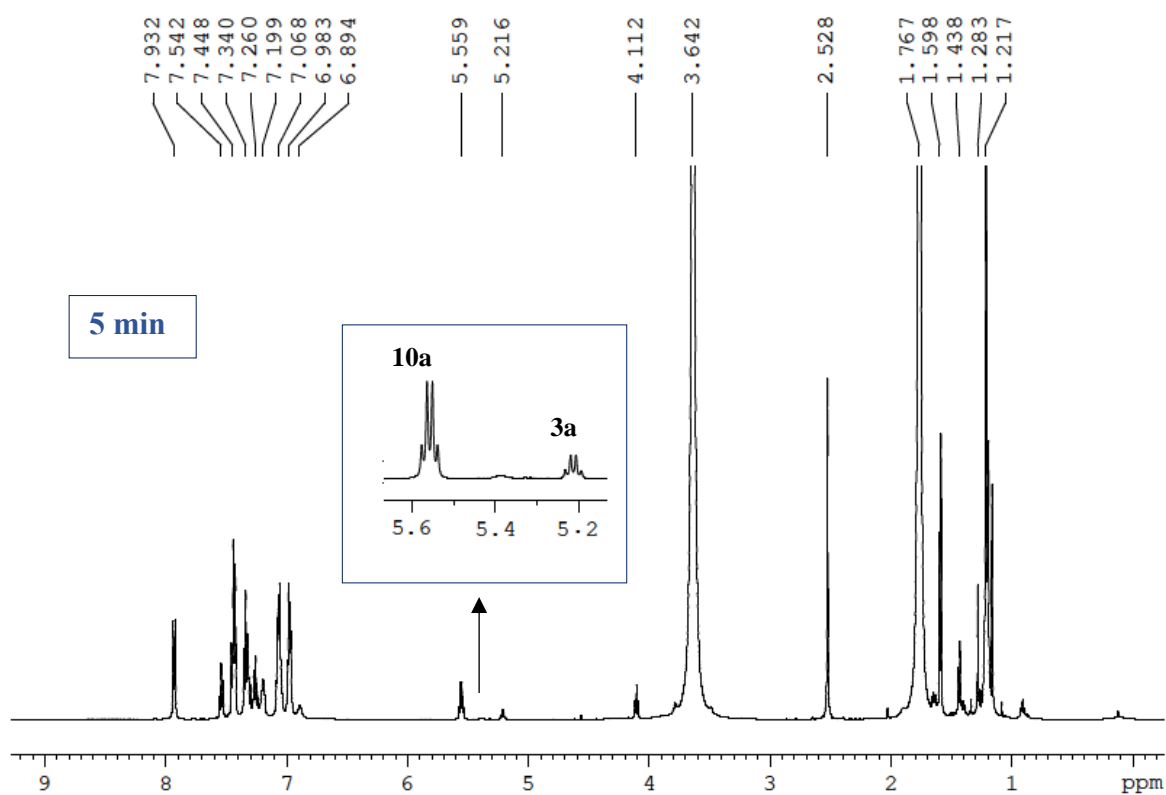


Figure S45. ^1H NMR spectra of competition reaction between HBcat and DBpin with acetophenone (5 min)

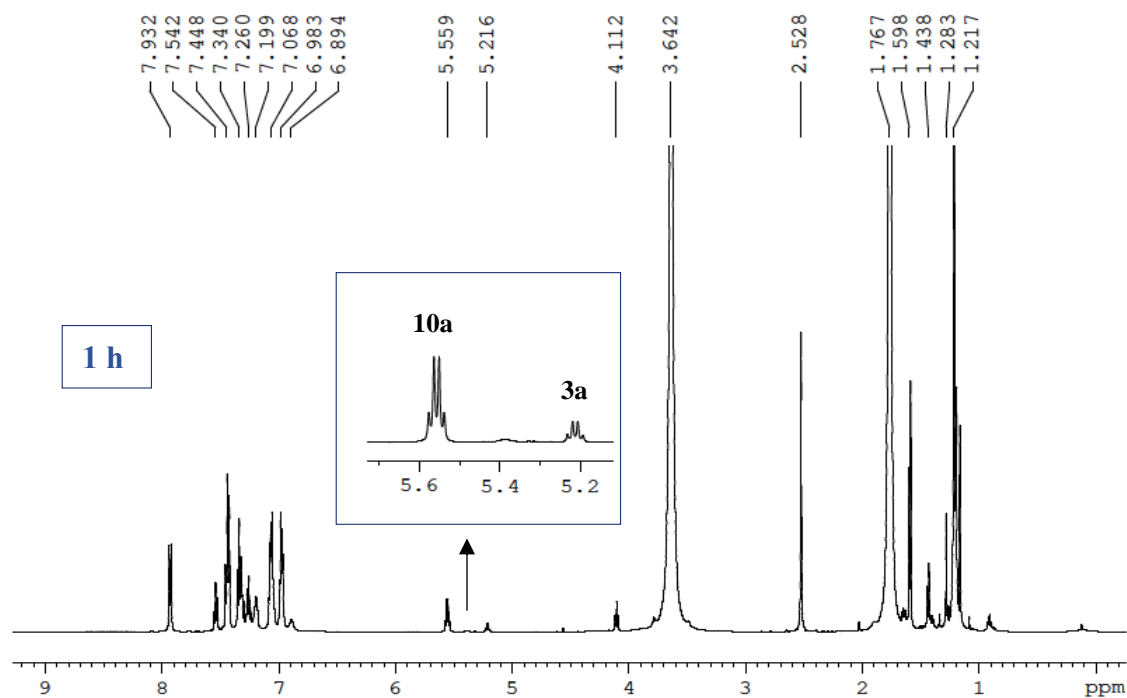


Figure S46. ^1H NMR spectra of competitive reaction between HBcat and DBpin with acetophenone (1 h)

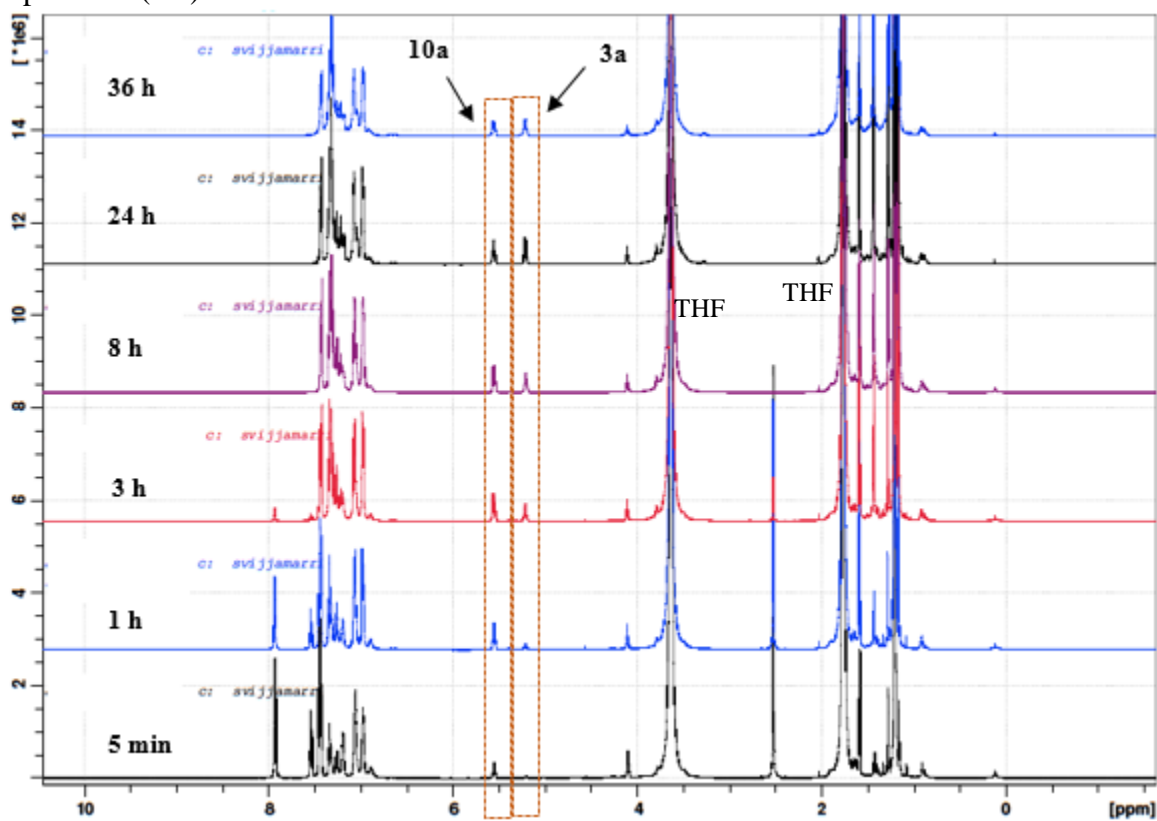


Figure S47. ^1H NMR spectra of competition reaction between HBcat and DBpin with acetophenone (5 min to 36 h)

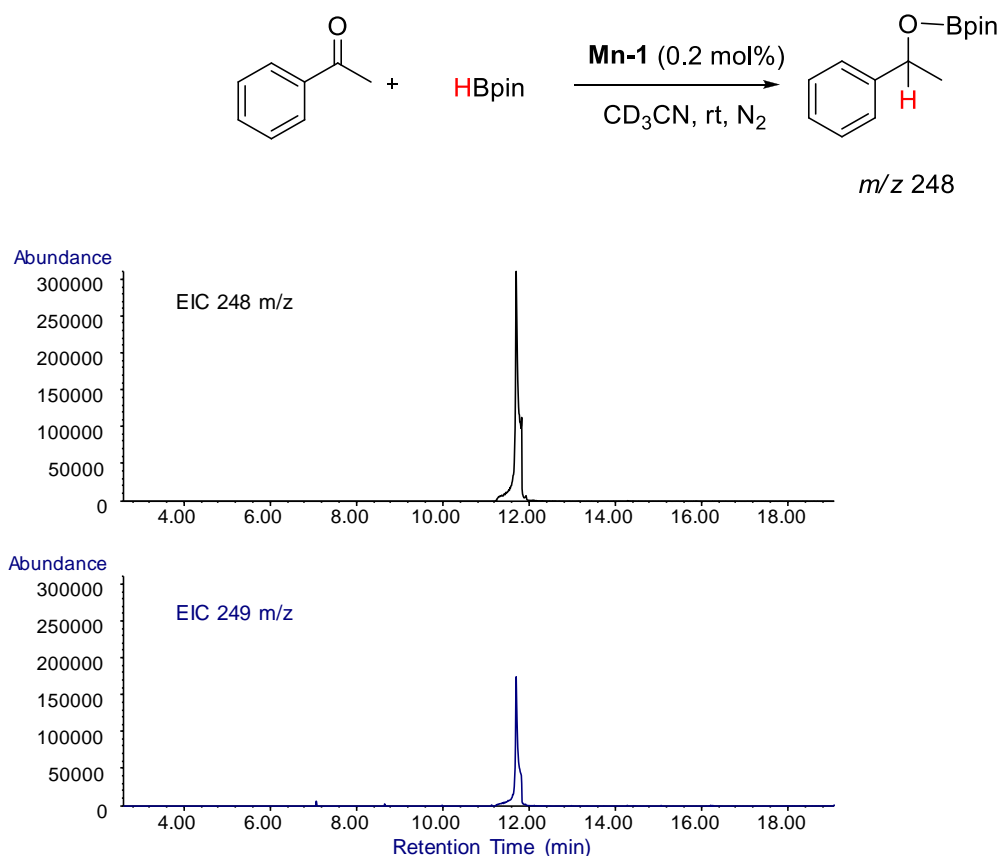


Figure S48. GC-MS extracted ion chromatograms of reaction between HBpin with acetophenone (for molecular ion $[M^+] = 248 \text{ } m/z$ and its $M+1$ peak of $249 \text{ } m/z$ occurring due to ^{13}C isotope corresponding to the presence of 14 carbon atoms).

Table S1 : GC-MS data extracted ion integration of HBpin-AcPh reaction

HBpin + AcPh Reaction						
Ion 248.00 (247.70 to 248.70)						
Peak #	Ret Time	Type	Width	Area	Start Time	End Time
1	11.702	VB	0.125	29851820	11.213	12.27
Ion 249.00 (248.70 to 249.70)						
Peak #	Ret Time	Type	Width	Area	Start Time	End Time
1	11.702	BB	0.097	4686981	11.206	11.998

Percentage of $249 \text{ } m/z$ in HBpin + AcPh reaction of $248 \text{ } m/z \sim 15.7 \%$

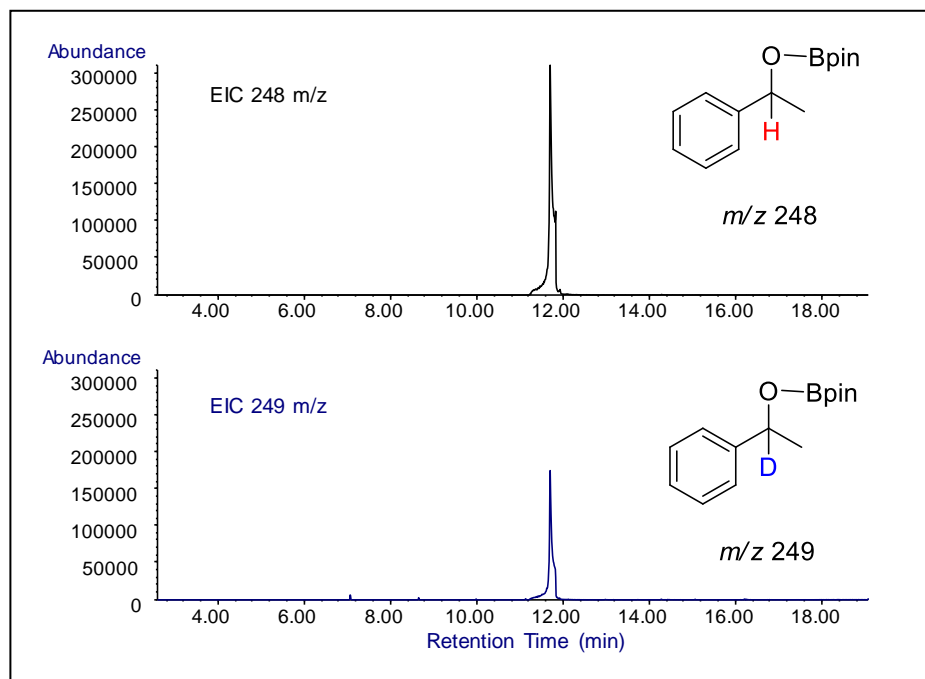


Figure S49. GC-MS extracted ion chromatograms of competition reaction between HBpin and DBpin with acetophenone

(Where molecular ion $[M^+] = 248\ m/z$ is formed by reaction with HBpin and peak of $249\ m/z$ may be attributed to reaction with DBpin as due to occurrence of ^{13}C isotope corresponding to the presence of 14 carbon atoms).

Table S2: GC-MS data integration of crossover experiment

HBpin + DBpin + AcPh Reaction						
Ion 248.00 (247.70 to 248.70)						
Peak #	Ret Time	Type	Width	Area	Start Time	End Time
1	11.71	BV	0.102	18437171	11.207	11.896
Ion 249.00 (248.70 to 249.70)						
Peak #	Ret Time	Type	Width	Area	Start Time	End Time
2	11.708	VV	0.067	8558193	11.533	11.908

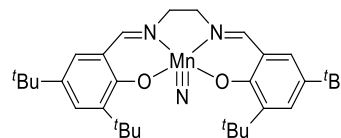
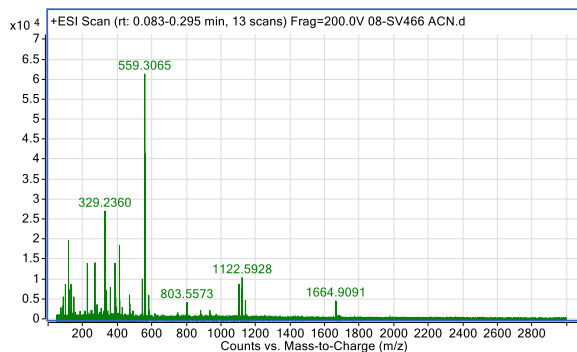
Percentage of m/z 249 (of m/z 248) with in HBpin + DBpin + AcPh Reaction = 46.41 %

The original isotopic **D** labelled product (m/z 249) is $46.41 - 15.70 = 30.71\ %$

The calculated H/D products ratio is thus approximately $69.3:30.7 \approx 2.3$

The ESI-HR-ToF-MS study of the reaction system was evaluated based on analysis of **Mn-1** alone (Fig. S50) and following the reaction with HBPIn in different ratios (Fig S51)

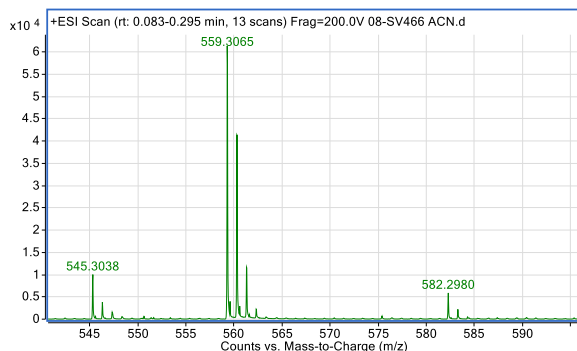
a)



$C_{32}H_{47}N_3O_2Mn$ $[M+H^+]$ mass
required 560.3048; mass found
560.3065

mass accuracy error 18 ppm

b)

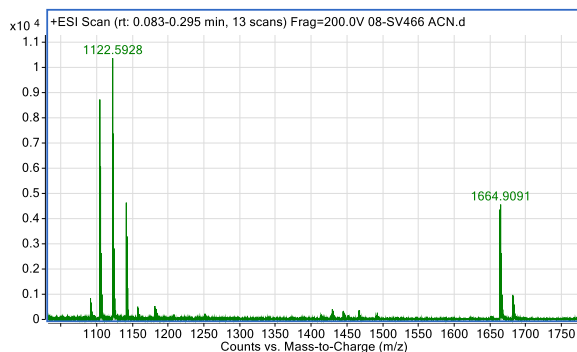


Mn₂ species

$C_{64}H_{96}N_6O_4Mn_2$ $[2M^+]$ mass required
1122.6249; mass found 1122.5928

M/z of 1104.6066 could be attributed
to a nitrogen-bridged dimer or loss of
water with mass errors of -15 ppm.

c)



Mn₃ species

$C_{96}H_{139}N_8O_6Mn_3$ mass required
1664.8959; mass found 1664.9091

Figure S50. ESI-ToF-MS of **Mn-1**

$C_{32}H_{46}N_3O_2Mn$ full mass range $[M^+]$ 559.2965, thus with mass accuracy errors of 18 ppm, and narrow mass range regions for monomer (a) and Mn_2 and Mn_3 species (b, c).

As shown in Fig. S51 below, no adduct of (salen)MnN-HBpin or (salen)Mn-HBpin was detected using the ESI-HR ToF MS. Similarly as for catalyst alone dimeric species could be observed in the region of m/z 1109 (**Mn-1** and HBpin 1:3), corresponding to a nitrogen bridged dinuclear species (Fig. S51). However, similar dinuclear species also showed up in the ESI of **Mn-1** alone without HBpin, but with 5 less mass units (m/z 1104, which could be assigned to a nitrogen bridged dimer), Fig. S51. We assume that the salen backbone hydrogenation, mostly likely at the imine double bond, could also take place under such conditions. When 1:1 ratio of **Mn-1**:HBpin was used, the dimeric species was observed at m/z 1107 (Fig. S51), likely due to a partial hydrogenation. In support of this, the imine peak of **Mn-1** at 8.02 ppm in ^1H NMR was observed to disappear when HBpin was added to the catalyst solution prepared with CDCl_3 at room temperature while other signals of **Mn-1** remained intact, at least initially.

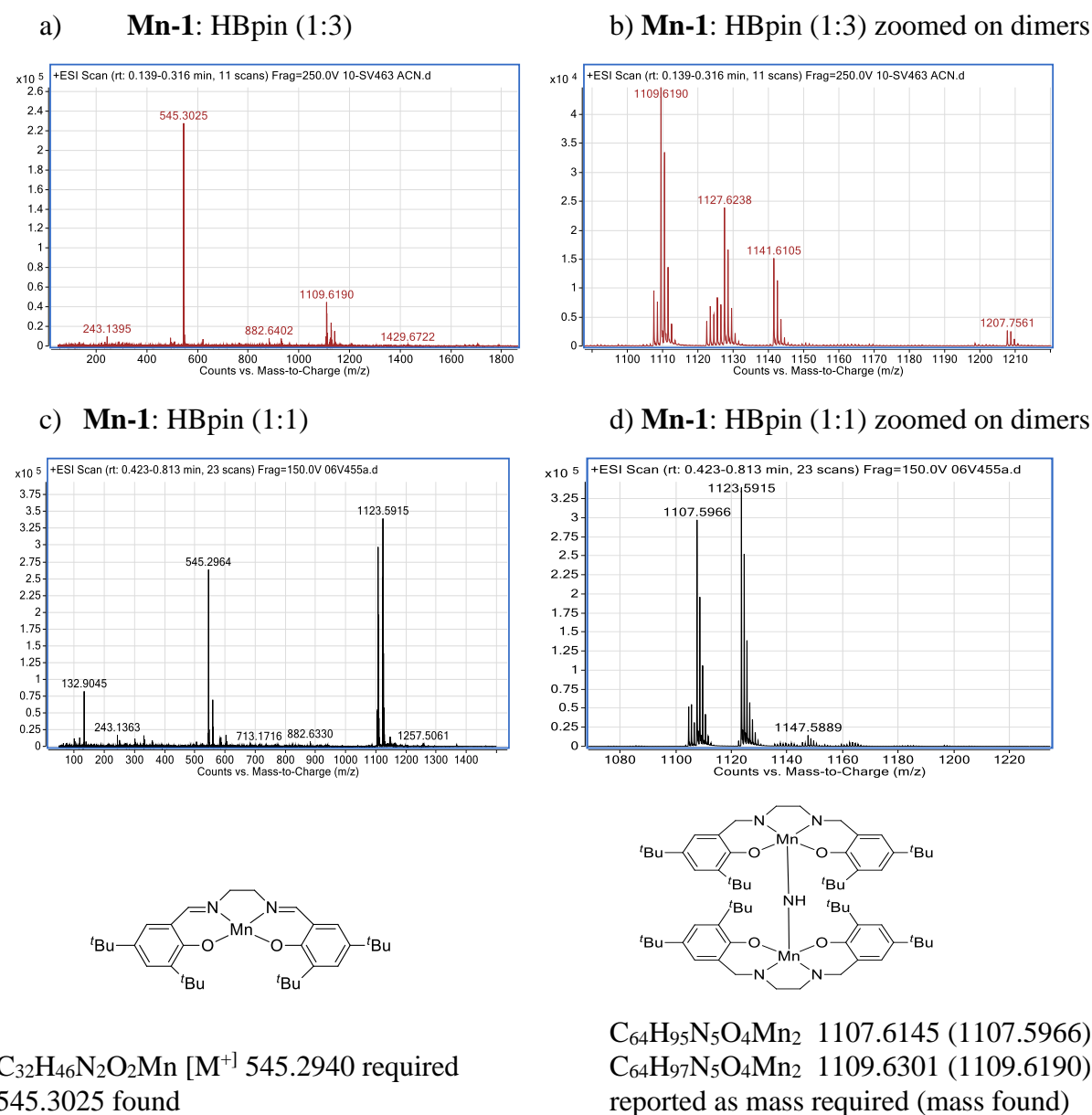


Figure S51. ESI-ToF-MS of reaction products for **Mn-1** with HBpin at different ratios

References

- 1 Tamang, S. R.; Findlater, M. *J. Org. Chem.* **2017**, *82*, 12857–12862.
- 2 Verma, P. K.; Sethulekshmi, A. S.; Geetharani, K. *Org. Lett.* **2018**, *20*, 7840–7845.
- 3 Wang, W.; Shen, X.; Zhao, F.; Jiang, H.; Yao, W.; Pullarkat, S. A.; Xu, L.; Ma, M. *J. Org. Chem.* **2018**, *83*, 69–74.
- 4 Zeng, H.; Wu, J.; Li, S.; Hui, C.; Ta, A.; Cheng, S. -Y.; Zheng, S.; Zhang, G. *Org. Lett.* **2019**, *21*, 401–406.
- 5 Zhang, G.; Zeng, H.; Wu, J.; Yin, Z.; Zheng, S.; Fettingner, J. C. *Angew. Chem. Int. Ed.* **2016**, *55*, 14369–14372.
- 6 V. K. Jakhar, M. K. Barman and S. Nembenna, *Org. Lett.*, 2016, **18**, 4710–4713.
- 7 Qi, X.; Zheng, T.; Zhou, J.; Dong, Y.; Zuo, X.; Li, X.; Sun, H.; Fuhr, O.; Fenske, D. *Organometallics* **2019**, *38*, 268–277.
- 8 Shin, W. K.; Kim, H.; Jaladi, A. K.; An, D. K. *Tetrahedron* **2018**, *74*, 6310–6315.
- 9 Panteleev, J.; Huang, R. Y.; Lui, E. K. J.; Lautens, M. *Org. Lett.* **2011**, *13*, 5314–5317.
- 10 Lessard, S.; Peng, F.; Hall, D. G. *J. Am. Chem. Soc.* **2009**, *131*, 9612–9613.